TGAL-92-05

PATH-CORRECTED BODY-WAVE MAGNITUDES AND YIELD ESTIMATES OF SEMIPALATINSK EXPLOSIONS

Rong-Song Jih and Robert A. Wagner

Teledyne Geotech Alexandria Laboratories
314 Montgomery Street
Alexandria, Virginia 22314-1581

APRIL 1992

SEMI-ANNUAL REPORT:	No. 1 (23 August 1991 - 4 April 1992)
ARPA ORDER NO.:	6731
PROJECT TITLE:	Statistical Study of Soviet Explosion Magnitudes and Yields Using Heavily Censored Historical Yields, Soviet-released Analog Waveforms, and Digital Data Recorded at Modern Arrays
CONTRACT NO.:	F29601-91-C-DB23

Approved for Public Release; Distribution Unlimited

Prepared for:
UNITED STATES AIR FORCE
AIR FORCE SYSTEM COMMAND
PHILLIPS LABORATORY (PL)
KIRTLAND AFB, NM 87117-6008

Monitored by:
DEFENSE ADVANCED RESEARCH PROJECTS AGENCY
NUCLEAR MONITORING RESEARCH OFFICE
3701 NORTH FAIRFAX DRIVE
ARLINGTON, VA 22203-1714

REPORT DOCUMENTATION PAGE

Form Approved
OMB No 0704-0188

1. AGENCY USE ONLY (Leave blank)	2. REPORT DATE	3. REPORT TYPE AND DATES COVERED
	4 April 1992	Semi-annual Report, 23 Aug 1991 - 4 April 1992

4. TITLE AND SUBTITLE

Path-corrected Body-wave Magnitudes and Yield Estimates of Semipalatinsk Explosions

5. FUNDING NUMBERS

Contract F29601-91-C-DB23

6. AUTHOR(S)

R.-S. Jih and R. A. Wagner

7. PERFORMING ORGANIZATION NAME(S) AND ADDRESS(ES)

Teledyne Geotech Alexandria Laboratory
314 Montgomery Street
Alexandria, VA 22314-1581

8. PERFORMING ORGANIZATION REPORT NUMBER

TGAL-92-05

9. SPONSORING/MONITORING AGENCY NAME(S) AND ADDRESS(ES)

DARPA/NMRO (Attn. Dr. Alan Ryall)
3701 North Fairfax Drive
Arlington, VA 22203-1714

10. SPONSORING/MONITORING AGENCY REPORT NUMBER

11. SUPPLEMENTARY NOTES

12a. DISTRIBUTION/AVAILABILITY STATEMENT

Approved for Public Release; Distribution Unlimited

12b. DISTRIBUTION CODE

13. ABSTRACT *(Maximum 200 words)*

Along with an extensive data set of worldwide explosions recorded at WWSSN, teleseismic short-period body-wave amplitudes from 92 Semipalatinsk explosions are measured and processed with an inversion scheme which simultaneously determines the the propagation path effect, the source size, and the receiver amplification. Partitioning a test site (such as Balapan) into several source regions according to the geological and geophysical characteristics and then applying the (highly regional) path corrections on top of the station corrections reduces the fluctuational variation across the network significantly, thereby resulting in a very favorable source estimator. For Semipalatinsk events in our WWSSN database, the new m_b factoring procedure provides more stable m_b measurements across the whole recording network with a reduction in the fluctuational variation by a factor of up to 3. The Kazakh-NTS m_b bias at 50 KT level is inferred as 0.36 magnitude unit. Based on the first motion of the P wave alone, our yield estimate of Soviet JVE (09/14/88) is 113 KT and that of the cratering event on 01/15/65 at Balapan test site is 111 KT, which are in excellent agreement with estimates derived by other means. A strong correlation between P–wave amplitude and L_g detection at teleseismic distance is also observed.

14. SUBJECT TERMS

Body-wave Magnitude, Yield Estimation, Station Amplification, Path Effect, m_b Bias, $m_b(L_g)$, General Linear Model, Maximum-likelihood Inversion

15. NUMBER OF PAGES

79

16. PRICE CODE

17. SECURITY CLASSIFICATION OF REPORT	18. SECURITY CLASSIFICATION OF THIS PAGE	19. SECURITY CLASSIFICATION OF ABSTRACT	20. LIMITATION OF ABSTRACT
Unclassified	Unclassified	Unclassified	UL

(THIS PAGE INTENTIONALLY LEFT BLANK)

Table of Contents

List of Figures

List of Figures

List of Tables

SUMMARY

The standard procedure used in estimating the source size of underground nuclear explosions using m_b measurements has been to separate the station terms from the network-averaged source terms. The station terms thus derived actually reflect the combination of the path effect and the station effect, when only those events in a close proximity are utilized. If worldwide explosions are used in the inversion, then the path effect tends to be averaged out at each station. In either case, the effect due to the propagation path alone would not be obvious.

Under this research contract **(F29601-91-C-DB23),** we propose to decompose the station amplification effect further with a joint inversion scheme which simultaneously determines the seismic source size, the path terms, and the receiver terms. Short-period *P*-wave amplitudes of 217 worldwide underground nuclear explosions, including 92 blasts from Semipalatinsk, recorded at 118 WWSSN stations have been used in one single inversion to infer the 2733 unknown parameters. For Semipalatinsk events in our WWSSN database, the new m_b factoring procedure provides more stable m_b measurements across the whole recording network with a reduction in the fluctuational variation by a factor of up to 3. A list of station corrections (which are applicable to all nuclear test sites around the world) and the path corrections for five Central Asian test sites is compiled. If WWSSN recordings of a new event become available, these corrections can be applied immediately without re-running the inversion in a batch mode.

We have recomputed the yield estimates of 92 Semipalatinsk explosions based on the path-corrected m_b values derived in this study. Based on the first motion of the *P* wave alone, the (central-value) yield estimate of Soviet JVE (09/14/88) is 113 KT and that of the cratering event on 01/15/65 at Balapan test site is 111 KT, which are in excellent agreement with estimates derived by other means. Thus the first motion of the initial short-period *P* waves appears to be a very favorable source measure for explosions fired in hard rock sites underlain by the stable mantle (such as Semipalatinsk). The m_b bias relative to NTS at 50KT level is inferred as 0.36 magnitude unit.

Also included in this *Semi-annual Report No. 1* is a preliminary assessment of WWSSN's capability in remotely monitoring Eurasian explosions. A strong correlation between the *P*–wave amplitude and L_g detection at teleseismic distance is observed. Further study along this line is needed to investigate its implication to low-yield threshold global monitoring.

(THIS PAGE INTENTIONALLY LEFT BLANK)

1. INTRODUCTION

The main problem with the conventional m_b is that it is a rather nebulous parameter; simply, it is a function of the largest peak-to-peak amplitude in the first few seconds of P wave motion with adjustment for the period of the arriving phase. The parameter m_b was adapted from the need to order systematically the size of earthquakes. The measure itself has inherent impreciseness as the measure is not related to the physics of the source *per se* but is the largest constructive interference of waves originating at the source, source region, propagation path, receiver region, and receivers (Butler, 1981; Johnson, 1981). To relate the m_b to the seismic yield, all effects not due to the source must naturally be corrected. It is often difficult, however, to separate these effects. In fact, the effects of source and propagation are often indistinguishable, and unless one is known the other cannot be uniquely determined (Johnson, 1981). Consequently, it was reported to be difficult to make m_b measurements that are internally consistent within 0.1 m_b with the conventional m_b (Bache, 1982), simply because some of the aforementioned effects are not accounted for accurately.

Von Seggern (1973) showed that including station corrections typically halves the standard deviation of m_b from North American LRSM stations recording NTS events. Even better results, with the standard deviation reduced by a factor of 3 or so, can be obtained for a network with all stations beyond 30°. Applying station corrections to the m_b determination or the network spectra averaging has become a standard procedure in this nuclear monitoring community (*e.g.*, Lilwall *et al.*, 1988; Murphy *et al.*, 1989; Sykes and Ekstrom, 1989; Jih and Shumway, 1989; and many others). The station effects are strongly dependent on azimuth (Chang and von Seggern, 1980), which led Bache (1982) and many others to believe that statistical station corrections will not be nearly so effective in reducing m_b variance in the multiple source region problem.

Marshall *et al.* (1979) attempted to correct several important factors that can bias m_b. They used bulletin log(A/T) data. These data are corrected for receiver-station attenuation differences, and the resulting magnitude is called m_2. Correcting m_2 for source-region attenuation gives m_3, and correcting m_3 for source depth gives m_Q. (The network averages of these m_bs are denoted by $\bar{m}_1$, $\bar{m}_2$, $\bar{m}_3$, and $\bar{m}_Q$, respectively.) The major change in this scheme is associated with the source-region correction, which can be as different as 0.4 m.u. between sites or a factor of about 2.5 in yield estimates. Essentially this approach is based on the discovery by Marshall and Springer (1976) and Douglas *et al.* (1981) that LRSM amplitude residuals correlate with P_n velocity near the stations and the assumption that such

correlation between the attenuation and P_n is valid elsewhere as well. However, it turns out that the standard deviation of the m_Q is not less than that for the m_1 and m_2 from the same data set (Marshall *et al.*, 1979; Bache, 1982).

It is obvious that the only way to reduce the statistical fluctuation is to obtain fundamental causal knowledge of the focusing and defocusing beneath the source and receiver. We expect teleseismic *P*-wave amplitudes to vary as the source location changes within a test site. The m_b residuals (with respect to the best-fitting m_b-yield curve) of NTS events show systematic trends that are consistent with local tectonics (Minster *et al.*, 1981). At Yucca Flat, the residuals are positive to the west and negative to the east of the north-south trending normal fault system that bisects the valley. At Pahute Mesa, the spatial pattern is less clear, but the residuals tend to be negative toward the center of the buried Silent Canyon Caldera and positive toward the edges. An attractive explanation is that these variations are due to focusing/defocusing effects that are not averaged out over the network, although the possibility of systematic source-coupling difference has not been eliminated.

Jih and Wagner (1991b, 1992) propose to compute the new station magnitude $m_{2.9}$ for the i-th event recorded at the j-th station as

$$m_{2.9}(i,j) = \log_{10}[A(i,j)/T(i,j)] + B(\Delta(i,j)) - S(i) - F(k(i),j)$$

where A(i,j) is the displacement amplitude (in millimicrons) and T(i,j) is the period (in seconds) of the *P* wave. The B(Δ) is the distance-correction term. S(j) is the station correction, and F(k(i),j) is the path correction for explosions from the k(i)-th source region. The resulting new magnitude is called $m_{2.9}$ to avoid confusion with the m_3 defined in Marshall *et al.* (1979) that corrects for the source-region attenuation and station terms solely based on published P_n velocity. The path corrections determined in this procedure provide direct and informative clues to characterize the various propagation paths. We will also use $m_{2.9}$ extensively throughout this study to characterize the magnitude-yield scaling relationship for Semipalatinsk explosions.

2. PATH-CORRECTED UNBIASED NETWORK m_b ESTIMATOR

The conventional definition of the station magnitude is computed as

$$m_b = \log_{10}(A/T) + B(\Delta) \qquad [1]$$

where A is the displacement amplitude (in nm) and T is the predominant period (in sec) of the *P* wave. The $B(\Delta)$ is the distance-correction term that compensates for the change of *P*-wave amplitudes with distance (*e.g.*, Gutenberg and Richter, 1956; Veith and Clawson, 1972). m_b in [1] is also denoted as m_1 in Marshall *et al.* (1979). The ISC bulletin m_b is just the network average of these raw station m_b values without any further adjustment.

Consider N_E explosions detonated at N_F source regions that are recorded at some or all of N_S stations. The conventional GLM [General Linear Model] or LSMF [Least Squares Matrix Factorization] network m_b (Douglas, 1966; Blandford and Shumway, 1982; Marshall *et al.*,1984; Jih and Shumway, 1989; Murphy *et al.*, 1989) is the least-squares or maximum-likelihood network average of the "station-corrected" magnitudes:

$$m_{2.2}(i,j) \equiv m_1(i,j) - S(j) \qquad [2]$$

where S(j) is the "statistical" or "empirical" receiver correction at the j-th station. In Marshall *et al.* (1979), *a priori* information about the P_n velocity underneath each station is used to determine its associated "deterministic" receiver correction, S(j), and the resulting magnitude is called m_2. The GLM receiver corrections, however, are inferred jointly from a suite of event-station pairs, and no *a priori* geophysical or geological condition is assumed (and hence the different notation $m_{2.2}$). The high correlation between the tectonic type and the GLM station terms suggests that the empirical station corrections do reflect the averaged upper mantle conditions underneath the receivers, if the azimuthal coverage at each station is broad enough.

Jih and Wagner (1991b, 1992) propose to compute the new station magnitude $m_{2.9}$ for the i-th event recorded at the j-th station as

$$m_{2.9}(i,j) \equiv m_1(i,j) - S(j) - F(k(i),j) = m_{2.2}(i,j) - F(k(i),j) \qquad [3]$$

At the j-th station, F(k(*),j) is a constant for all events detonated in the same k-th "geologically and geophysically uniform region". Partitioning a single nuclear test site into several "regions" may be necessary in order to account accurately for the focusing/defocusing effects. This $m_{2.9}$ is very similar to the m_3 in Marshall *et al.* (1979) except that, again, *a priori* attenuation information of the source region is used in Marshall *et al.* (1979) to determine the

correction term, whereas Jih and Wagner (1991a, 1991b, 1992) invert for the path or near-source effects from the data empirically. In other words, the source-region corrections proposed by Marshall *et al.* (1979) are constants (for all explosions in the same source region) regardless of the location of the seismic stations, whereas the path or near-source corrections in Equation [3] are highly dependent on the source-station paths.

We now examine briefly the fundamental difference between the present scheme (Equation [3]) and the previous GLM schemes. In LSMF and the standard GLM schemes (*e.g.*, Douglas, 1966; Blandford and Shumway, 1982; Marshall *et al.*, 1984; Lilwall *et al.*, 1988; Jih and Shumway, 1989; Murphy *et al.*, 1989), it is assumed that the observed station m_b(i,j) is the sum of the true source size of the i-th event, E(i), the receiver term of the j-th station, S(j), and the random noise, v(i,j):

$$m_b(i,j) = E(i) + S(j) + v(i,j) \qquad [4]$$

The receiver term, S(j), is constant with respect to all explosions from different test sites, and hence it would inherently reflect the "averaged" receiver effect --- provided the paths reaching the station have broad azimuthal coverage. When world-wide explosions are used, the standard deviation (σ) of the noise v in [4] is typically about 0.3 m.u. or larger.

If LSMF or GLM is applied to events within a smaller area of source region, then the σ of v in [4] could reduce to 0.15-0.2 m.u. However, the result of such "single-test-site GLM" approach should be interpreted or utilized cautiously. The event m_b values (*i.e.*, the "E" term in [4]) so determined are excellent estimates of "relative source size" for that test site only. If this "single-test-site GLM" inversion is applied to several test sites separately, it may not be easy or obvious to find a consistent baseline for "absolute yield" estimation or immediate combination of the (inter-site) magnitudes, since the recording network is typically different from one test site to another, and hence the station terms are inevitably inconsistent. Furthermore, the station terms derived by the "single-test-site GLM" may not necessarily represent the attenuation underneath the receiver side alone. They could be "contaminated" or sometimes even overwhelmed by the path/near-source effects shared by the explosions confined in a narrow azimuthal range. This could explain the once puzzling and controversial phenomenon Butler and Ruff (1980) (also Butler, 1981; Burdick, 1981) reported, namely that using Soviet explosions from one test site alone may fail to discern the attenuation differential between the eastern and western U.S. There is no doubt, however, that the GLM or LSMF type of methodology can infer the station terms which are strongly correlated with the upper mantle attenuation underneath the stations, provided the seismic sources have a broad spatial coverage as did those in North (1977), Douglas and Marshall (1983), Lilwall and Neary

(1985), Ringdal (1986), Jih and Wagner (1991b, 1992), and many others.

In the present scheme ([3]), however, we reformulate the whole model as

$$m_b(i,j) = E(i) + S(j) + F(k(i),j) + v(i,j) \qquad [5]$$

where F(k(i),j) is the correction term at the j-th station for the propagation effect or the near-source focusing/defocusing effect, which is constant for all events in the k-th "geologically and geophysically uniform region". For each seismic station, this F can be regarded as its azimuthal variation around the mean station term S. However, as explained previously, it would be more appropriate to consider F the path or near-source term because the back azimuths at the station could be nearly identical for adjacent test sites (such as Degelen and Murzhik), and yet the "F" terms could be very different. By incorporating the F term into the model, the σ for world-wide explosions is reduced to about 0.2, roughly the same level that which a "single-test-site GLM" could achieve. Intuitively, the present scheme (Equations [3] or [5]) provides a more detailed (and hence better) model than that of Equation [4] in describing the whole propagation path from the source towards the receiver. Simply put, Equation [4] yields a stronger fluctuation in the source terms, E, as well as a larger standard deviation of v because each term in the right-hand side of Equation [4] would have to "absorb" part of the missing F term in [5]. This is exactly the same reason why $m_{2.2}$ has smaller variation than m_1.

Roughly speaking, the procedure described in [3] has the following advantages:

- It provides more stable m_b measurements across the whole recording network, as compared to the conventional GLM or LSMF procedure which only corrects for the station terms. The reduction in the standard deviation of network m_b from $\overline{m}_1$ to $\overline{m}_{2.9}$ could reach a factor of nearly 3. As a result, the scatter in $\overline{m}_{2.9}$ versus log(yield) is smaller than that for other m_b.
- The resulting network m_b values are not significantly different from the GLM results. Thus if the network m_b values derived by GLM or LSMF are unbiased, so are the refined results.
- The separation of the path effect from the station effect is a crucial step to study the various propagation phenomena, which in turn would improve our understanding of the seismic source as well.

We have applied this procedure to 217 worldwide explosions, and the resulting $\overline{m}_{2.9}$ values of 92 Semipalatinsk explosions are listed in Table 1. The 118 WWSSN [World Wide Standarized Seismograph Network] stations are selected such that each station records 10 or

more good explosion signals. There are 13840 signals, 9080 noise measurements, and 1609 clips from 17 test sites that are used to invert for the 2733 unknown parameters with the maximum-likelihood approach. The standard deviation of v(i,j) in [5] is 0.196, as compared to 0.294 if the conventional GLM (Equation [4]) is applied to the same data set. A list of the event magnitudes and the path corrections for northern test site in Novaya Zemlya has been presented in Jih and Wagner (1992). Here we limit the discussion to Semipalatinsk explosions only. The $m_b(P_{max})$ of 25 Balapan events for which the $m_b(P_b)$ and $m_b(P_a)$ are missing are based on station m_b values published by Lilwall *et al.* (1988). For these station m_b values, a compensating correction to convert the B(Δ) (*cf.* Equation [1]) of Gutenberg and Richter (1956) to that of Veith and Clawson (1972) is applied to every station m_b before these recordings are incorporated into our data set.

Table 1. Magnitudes of Semipalatinsk Explosions							
Event		# of Signals	Magnitudes [$m_{2.9}$]				Yield
Date	Site[1]	Ns Nn Nc[2]	S.E.M.[3]	P_a	P_b	P_{max}	
650115B	BTZ	45 1 2	0.028	5.473	5.709	5.865	100-150
651121D	Deg	48 15 1	0.024	4.962	5.240	5.452	29
660213D	Deg	51 4 10	0.024	5.717	5.965	6.152	125
660320D	Deg	49 9 8	0.024	5.416	5.697	5.916	100
660507D	Deg	9 26 1	0.033	4.089	4.237	4.529	4
661019D	Deg	51 10 5	0.024	5.164	5.423	5.596	20-150
661218M	Mzk	55 8 1	0.024	5.395	5.632	5.852	20-150
670226D	Deg	48 9 6	0.025	5.438	5.688	5.914	20-150
670916M	Mzk	36 29 2	0.024	4.657	4.937	5.182	<20
670922M	Mzk	35 31 1	0.024	4.516	4.840	5.118	10
671122M	Mzk	7 63 0	0.023	____	3.975	4.353	<20
680619B	BNE	28 3 2	0.034	4.666	5.002	5.256	<20
680929D	Deg	50 7 6	0.025	5.222	5.511	5.710	60
690531M	Mzk	30 30 0	0.025	4.468	4.885	5.115	<20
690723D	Deg	38 20 1	0.025	4.711	5.022	5.248	16
690911D	Deg	19 38 0	0.026	4.141	4.381	4.709	<20
691130B	BTZ	49 0 0	0.028	5.362	5.733	5.915	125
691228M	Mzk	45 9 3	0.026	5.264	5.551	5.753	46
700721M	Mzk	38 20 1	0.025	4.689	5.033	5.281	<20
701104M	Mzk	38 22 1	0.025	4.934	5.137	5.349	<20
710322D	Deg	43 14 3	0.025	5.117	5.408	5.587	20-150
710425D	Deg	37 5 0	0.030	5.434	5.696	5.891	90
710606M	Mzk	38 12 2	0.027	4.879	5.218	5.425	16

1) BSW = SW subsite, Balapan; BNE = NE subsite, Balapan; BTZ = transition zone, Balapan; Deg = Degelen Mountain; Mzk = Murzhik.

2) Ns = # of signals, Nn = # of noise measurements, Nc = # of clips.

3) standard error in the mean.

Table 1. Magnitudes of Semipalatinsk Explosions (continued)							
Event		# of Signals	Magnitudes [$m_{2.9}$]				Yield
Date	Site	Ns Nn Nc	S.E.M.	P_a	P_b	P_{max}	
710619M	Mzk	41 13 0	0.027	4.863	5.162	5.392	<20
710630B	BTZ	31 19 1	0.027	4.448	4.766	5.036	<20
711009M	Mzk	27 12 3	0.030	4.791	5.026	5.226	12
711021M	Mzk	32 9 0	0.031	4.875	5.208	5.442	23
711230D	Deg	16 3 0	0.045	5.080	5.425	5.610	20-150
720210B	BNE	34 8 2	0.029	4.811	5.073	5.306	16
720328D	Deg	28 17 0	0.029	4.481	4.826	5.051	6
720816D	Deg	23 23 1	0.029	4.447	4.735	4.991	8
720826M	Mzk	29 15 2	0.029	4.688	5.033	5.258	<20
720902M	Mzk	15 29 0	0.029	4.148	4.405	4.682	2
721102B	BSW	42 1 15	0.026	5.619	5.935	6.158	165
721210D	Deg	30 7 5	0.030	5.075	5.402	5.624	20-150
721210B	BNE	44 2 11	0.026	____	5.801	5.998	140
730723B	BTZ	52 1 1	0.027	5.743	5.985	6.171	___
731214B	BNE	49 8 6	0.025	5.248	5.549	5.760	___
750427B	BNE	18 1 1	0.044	4.904	5.238	5.521	___
760704B	BTZ	38 0 5	0.030	5.199	5.545	5.812	___
761123B	BNE	22 0 0	0.042	____	____	5.680	___
761207B	BSW	17 2 1	0.044	4.928	5.351	5.581	___
770329D	Deg	25 14 0	0.031	4.401	4.785	5.073	___
770730D	Deg	21 16 0	0.032	4.296	4.692	4.943	___
780326D	Deg	25 6 0	0.035	4.995	5.301	5.530	___
780422D	Deg	21 9 0	0.036	4.562	4.821	5.071	___

Table 1. Magnitudes of Semipalatinsk Explosions (continued)							
Event		# of Signals	Magnitudes [$m_{2.9}$]				Yield
Date	Site	Ns Nn Nc	S.E.M.	P_a	P_b	P_{max}	
780611B	BSW	17 0 1	0.046	5.246	5.513	5.811	___
780705B	BSW	38 7 7	0.027	5.215	5.489	5.738	___
780728D	Deg	36 9 6	0.027	5.068	5.365	5.577	___
780829B	BNE	16 0 0	0.049	____	____	5.926	___
780915B	BTZ	36 1 6	0.030	5.414	5.655	5.828	___
781104B	BNE	40 9 6	0.026	5.109	5.349	5.566	___
781129B	BSW	28 0 0	0.037	____	____	5.886	___
790623B	BTZ	40 2 3	0.029	5.639	5.878	6.084	___
790707B	BNE	30 0 0	0.036	____	____	5.812	___
790804B	BSW	40 4 20	0.024	5.609	5.894	6.114	HE*
790818B	BNE	28 0 0	0.037	____	____	6.095	___
791028B	BNE	44 5 13	0.025	5.463	5.700	5.932	HE
791202B	BSW	15 0 0	0.050	____	____	5.900	___
791223B	BSW	40 3 17	0.025	5.599	5.890	6.139	HE
800522D	Deg	36 22 1	0.025	4.721	4.980	5.188	___
800629B	BSW	46 5 6	0.026	5.202	5.455	5.664	___
800914B	BTZ	34 5 6	0.029	5.493	5.824	6.087	___
801012B	BNE	23 0 0	0.041	____	____	5.856	___
801214B	BTZ	28 0 0	0.037	____	____	5.919	___
801227B	BNE	24 0 0	0.040	____	____	5.899	___
810422B	BSW	25 0 0	0.039	____	____	5.922	___
810913B	BTZ	17 0 0	0.047	____	____	6.077	___
811018B	BSW	41 3 7	0.027	5.492	5.778	5.989	HE

*: a historical event discussed at U.S.-U.S.S.R. negotiation.

Table 1. Magnitudes of Semipalatinsk Explosions (continued)							
Event		# of Signals	Magnitudes [$m_{2.9}$]				Yield
Date	Site	Ns Nn Nc	S.E.M.	P_a	P_b	P_{max}	
811129B	BSW	37 11 5	0.027	5.044	5.313	5.527	___
811227B	BSW	23 0 0	0.041	____	____	6.196	___
820425B	BTZ	14 0 0	0.052	____	____	5.970	___
820704B	BTZ	21 0 0	0.043	____	____	6.054	___
820831B	BSW	27 17 1	0.029	4.559	4.865	5.097	___
821205B	BSW	26 0 0	0.038	____	____	6.108	___
821226B	BNE	38 10 1	0.028	5.171	5.378	5.606	___
830612B	BTZ	16 0 0	0.049	____	____	5.940	___
831006B	BSW	25 0 0	0.039	____	____	5.939	___
831026B	BTZ	18 0 0	0.046	____	____	5.989	___
831120B	BNE	17 8 3	0.037	4.933	5.130	5.339	___
840425B	BTZ	21 0 0	0.043	____	____	5.895	___
840526B	BNE	31 0 3	0.034	5.547	5.848	6.005	HE
840714B	BTZ	22 0 0	0.042	____	____	6.057	___
841027B	BSW	19 0 0	0.045	____	____	6.233	___
841202B	BNE	22 0 0	0.042	____	____	5.709	___
841216B	BTZ	15 0 0	0.050	____	____	6.038	___
841228B	BSW	19 0 0	0.045	____	____	5.924	___
850210B	BSW	18 1 4	0.041	5.309	5.585	5.834	___
850615B	BSW	15 0 0	0.050	____	____	6.060	___
850630B	BSW	37 3 6	0.029	5.406	5.679	5.898	___
870620B	BSW	24 3 13	0.031	5.520	5.766	5.999	___
880914B	BSW	25 0 1	0.038	5.480	5.777	6.021	JVE*

*: Joint Verification Experiment.

3. RECEIVER AND PATH EFFECTS ON P WAVES FROM SEMIPALATINSK

Figure 1 shows our receiver terms which are inferred jointly along with the source-size estimates and path terms from the worldwide explosions (top) along with the the deterministic station terms predicted by Marshall *et al.* (1979) based on published P_n velocity around the world (bottom). The receiver corrections derived with our approach match the average tectonic structure underneath each station very well, mainly due to the broad coverage of azimuths at each station. Generally speaking, the station terms are positive in shield regions such as Australia, Canada, India, and Scandinavia, and they are negative in the east Africa rift valleys, mid-ocean ridges (*e.g.*, Iceland and Azores Islands), island arcs (*e.g.*, Indonesia, Japan, and Taiwan), and Himalaya Mountain Ranges (Chaman Fault, northern India, Nepal, and Burman Arc). Solomon and Toksoz (1970) and many other studies (*e.g.*, Evernden and Clark, 1970; Booth *et al.*, 1974) found that for stations in U.S., the attenuation is higher between the Rockies and Cascades, and in the northeastern U.S. This pattern is also observable in Figure 1 (see also North, 1977). As North (1977) put it, it is gratifying that a simple parameter such as m_b can be utilized to reveal the tectonics. It should be noted, however, that our empirical station terms also include the effect due to the crustal amplification if such local site effect is shared by all ray paths from different test sites to a particular station. This could be the reason of a few outliers such as HNR (Honiara, Solomon Islands), PMG (Port Moresby, East Papua New Guinea), RAB (Rabaul, New Britain), and BAG (Baguio City, Luzon, Philippines) which do not show negative station terms as would be expected from the strong seismicity in that region (*cf.* Figure 1). Another possible reason is that these stations have relatively poorer azimuthal sampling in our data set, and hence the station bias at these three stations is not well constrained. The minor discrepancy between the deterministic corrections by Marshall *et al.* (1979) and our empirical corrections could be due to the same reason.

Figure 2 shows the empirical station terms determined by North (1977) and Ringdal (1986) with ISC recordings of world-wide earthquakes occurred during the periods of 1964-1973 and 1971-1980, respectively. After the mean station residual of 0.104 m.u. is removed from Ringdal's station terms, the spatial pattern of his corrections appears to be in very good agreement with that of North (1977) and the present study.

Figures 3 through 7 show the map of the "pure propagation effect" (top) and the combined station amplification (bottom) defined as the sum of the receiver term and the path effect for explosions detonated in five source regions in Eastern Kazakhstan which include

Degelen Mountain [Deg] and Murzhik [Mzk] in addition to the three subregions defined in Ringdal and Marshall (1989): southwestern Balapan [BSW], northeastern Balapan [BNE], and the transition zone [BTZ] between BSW and BNE. The path term at each station can be regarded as the azimuthal variation (towards the various source regions) relative to the averaged station amplification. An important observation is that all these five test sites exhibit very different azimuthal and radial amplitude variations. Degelen and Murzhik events are systematically enhanced in the western U.S. and reduced in eastern U.S., whereas Balapan events are all reduced in the whole U.S. Murzhik events are reduced in Scandinavia, but Balapan and Degelen events get enhanced there. Such highly direction-dependent, distance-dependent, and site-dependent patterns of the amplitude fluctuation could be a diagnostic for the path effects in the proximity of the test sites. Back projections (*e.g.*, Lynnes and Lay, 1990) of the m_b residuals onto the upper mantle and the lower crust reveal that similar m_b residuals come into alignment in several regions partitioned by known geological features (Jih and Wagner, 1991a). Murzhik events recorded in the western U.S. and in northeast Asia, Degelen events in the western U.S., and SW Balapan events at western European stations must pass through the area between Chinrau fault and Chingiz-Kalba shear zone. All these paths show positive m_b residuals. The area north of Chinrau fault might have some complex features that result in negative mean m_b residuals. Paths from NE Balapan to North America and many continental European stations must cross this area or even travel along the Chinrau fault before entering the deeper mantle, and hence the complexity in the waveforms is inevitable. It seems that the mean m_b–L_g separation of 0.11-0.17 m.u. (*e.g.*, Ringdal and Hokland, 1987; Ringdal and Marshall, 1989; Richards *et al.*, 1990; Jih and Wagner, 1991a) between the NE and SW subregions of Balapan could be due in part to the path effects --- in addition to the difference of source medium postulated previously by Marshall *et al.* (1984). A detailed discussion on the seismic variability within Balapan test site is given in a later section (*cf.* pages 48-49). Path effects can also explain why the SW Balapan waveforms tend to be more complex at YKA than those recorded at WRA, EKA, and GBA arrays (Jih and Wagner, 1991a).

The initial *P* waves from the three adjacent test sites have virtually the same incident angle at each teleseismic station, and anything in common across all events (such as the crustal amplification as well as the upper mantle attenuation underneath the receiver) would have been lumped into the constant station term. Thus the station residuals averaged over all events from the same test site would correlate very little with the receiver. Instead, they should reveal more site-dependent information about the focusing/defocusing pattern underneath E. Kazakhstan.

The largest and most prominent fault in the region is the southeast-trending Chingiz right-lateral strike-slip fault that passes about 10 km southwest of Degelen Mountain and right across the Murzhik test area (Rodean, 1979; Bonham *et al.*, 1980; Leith, 1987b). Soviets reported that this fault has a very steep dip, which is consistent with its linear expression over large distance as seen on Landsat imagery (Bonham *et al.*, 1980). A distinct fault-line scarp is developed along much of the oldest metamorphic rocks. Chingiz Fault extends for a total length of about 700 km. Soviet reports postulate that this fault extends down to the boundary of the granite layer of the crust and possibly into the upper mantle. For Murzhik explosions, the propagation of P_n and L_g waves could be affected by this fault significantly, which results in a radiation pattern such as we observe in Figure 7. More specifically, the rays towards NW direction could be reflected or diffracted to other quadrants, due to its post-critical incidence angles. Such relatively distant crustal structure should have little impact on the first P waves of Balapan explosions at teleseismic distances, however. As a result, amplitudes of Balapan events recorded at Scandinavian stations are still largely controlled by the weak-attenuating shield paths.

Table 2 lists the WWSSN station corrections and path corrections for explosions in the five Central Asian nuclear test sites. Note that the station terms are applicable to other source regions of the world as well.

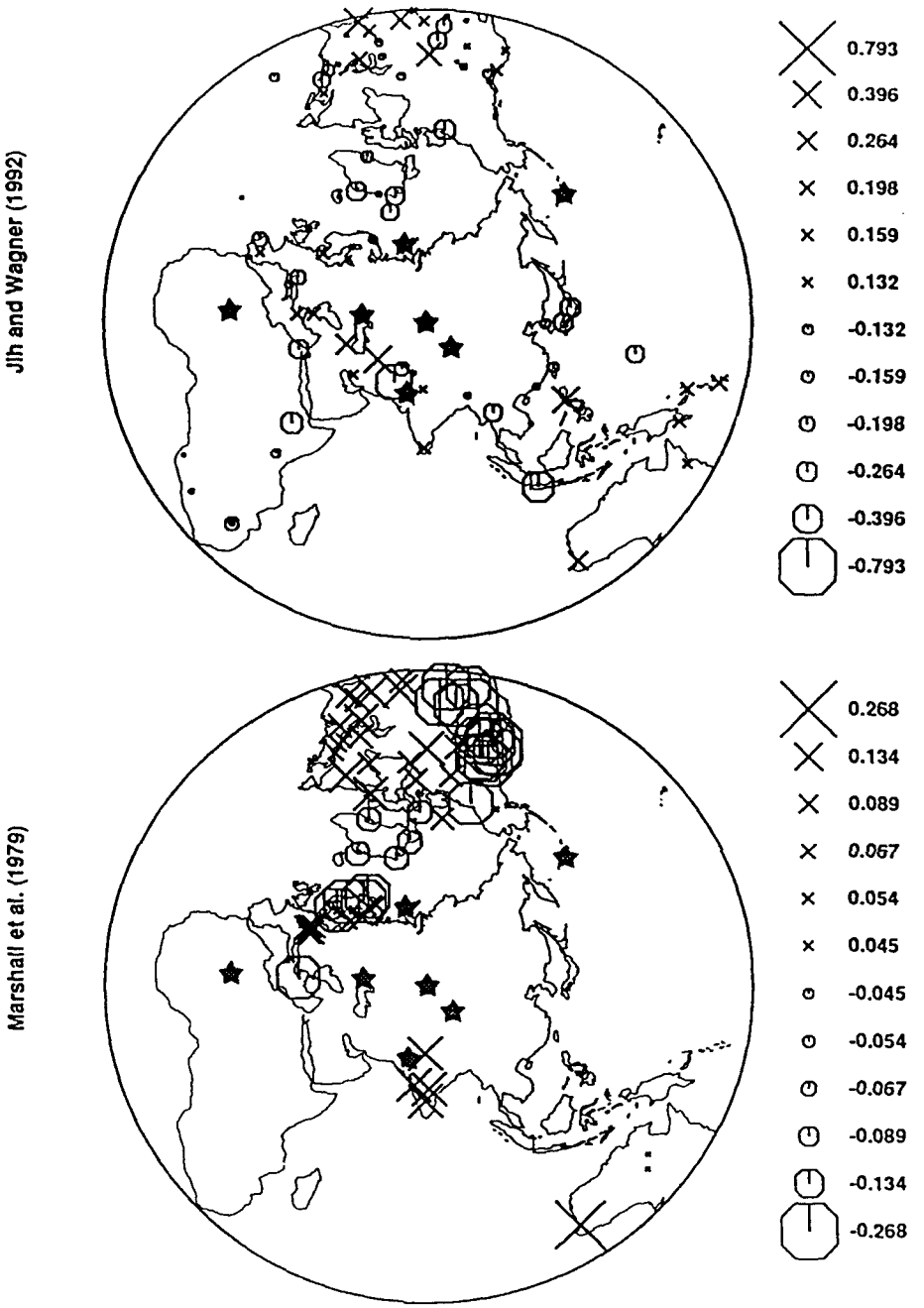

EMPIRICAL STATION TERMS VS. DETERMINISTIC STATION TERMS

Figure 1. The WWSSN station terms (top) inferred from a GLM/MLE joint inversion scheme which simultaneously inverts for the seismic source sizes, receiver terms, as well as the path effects. The inversion of 2733 unknown parameters is carried out with 13840 signals, 9080 noise measurements, and 1609 clips from 217 worldwide explosions recorded at 118 selected WWSSN stations. Only paths within 20 and 95 degrees are used. The high correlation between the tectonic type and the station terms suggests that these empirical corrections do reflect the upper mantle conditions underneath the receivers. Darkened stars represent some of the nuclear test sites used in this study. The match between the deterministic station corrections derived by Marshall *et al.* (1979) (bottom) and our empirical corrections is fairly good.

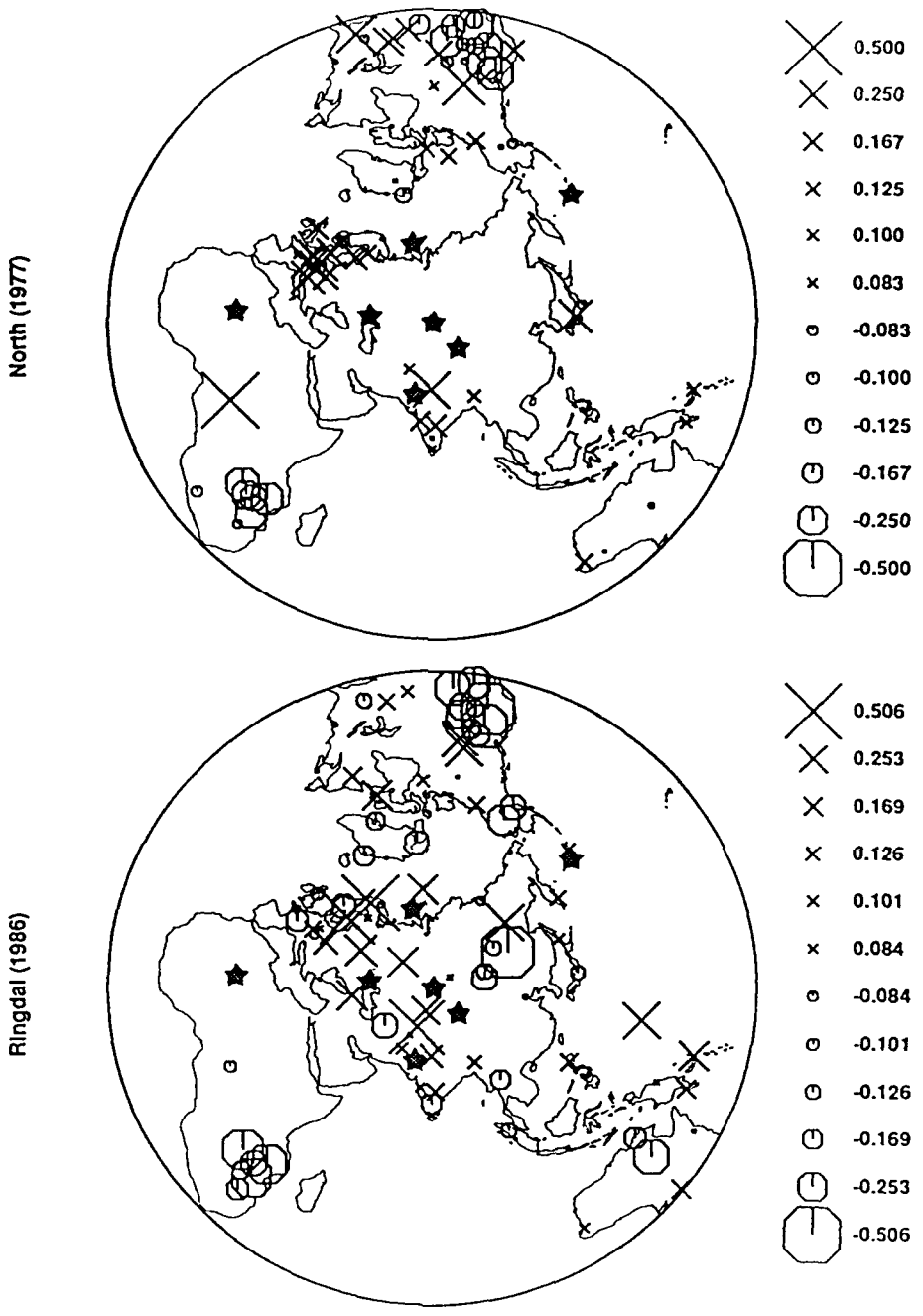

Figure 2. The empirical station terms determined by North (1977) and Ringdal (1986) with world-wide earthquakes recorded at ISC during the periods of 1964-1973 and 1971-1980, respectively. After the mean station residual of 0.104 m.u. is removed from Ringdal's station terms, the spatial pattern of his corrections appears to be in very good agreement with that of North (1977) and the present study.

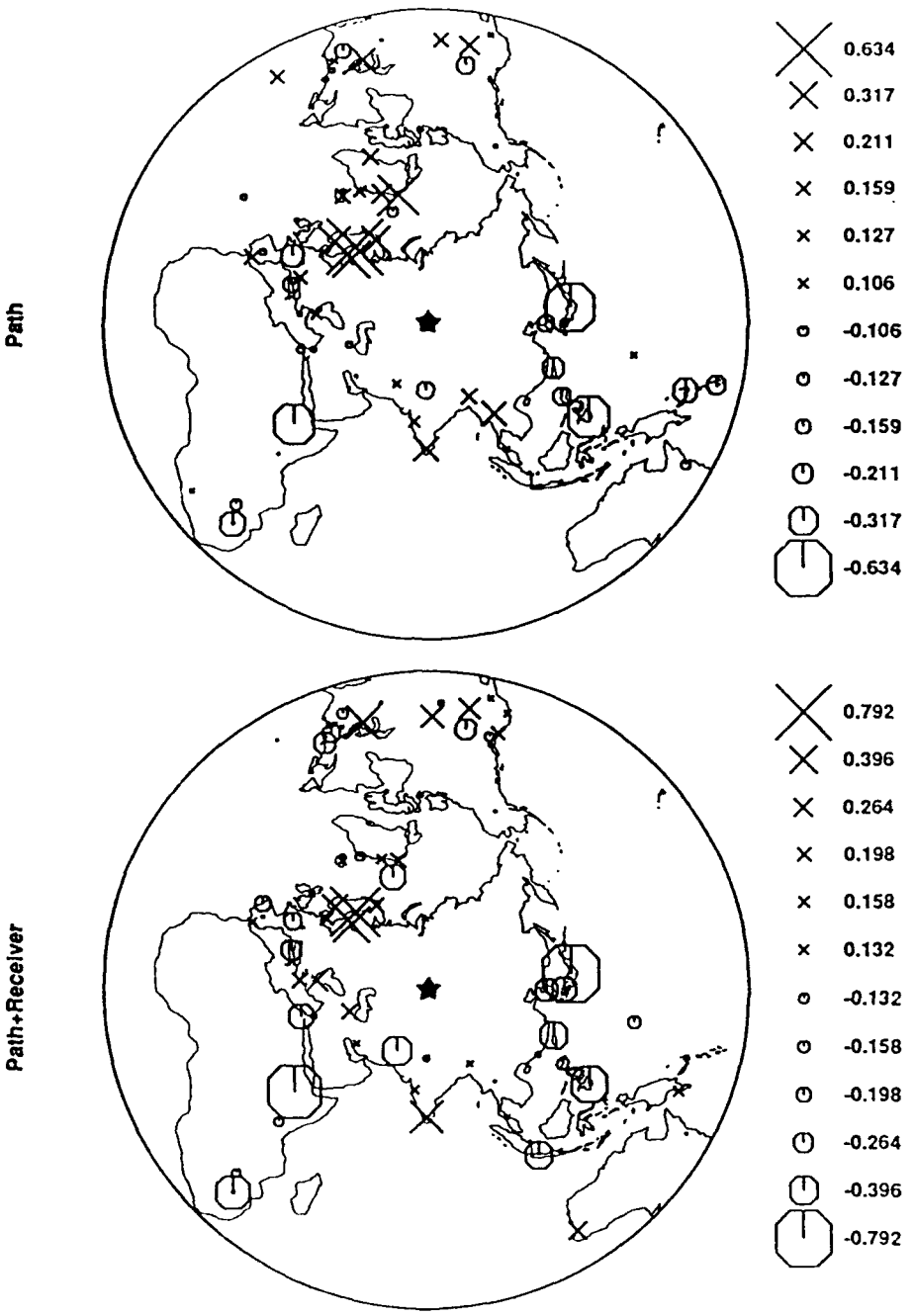

Figure 3. The map showing the "pure propagation effect" (top) and the combined station amplification (bottom) defined as the sum of the receiver term (Figure 1) and the path effect for southwestern Balapan explosions.

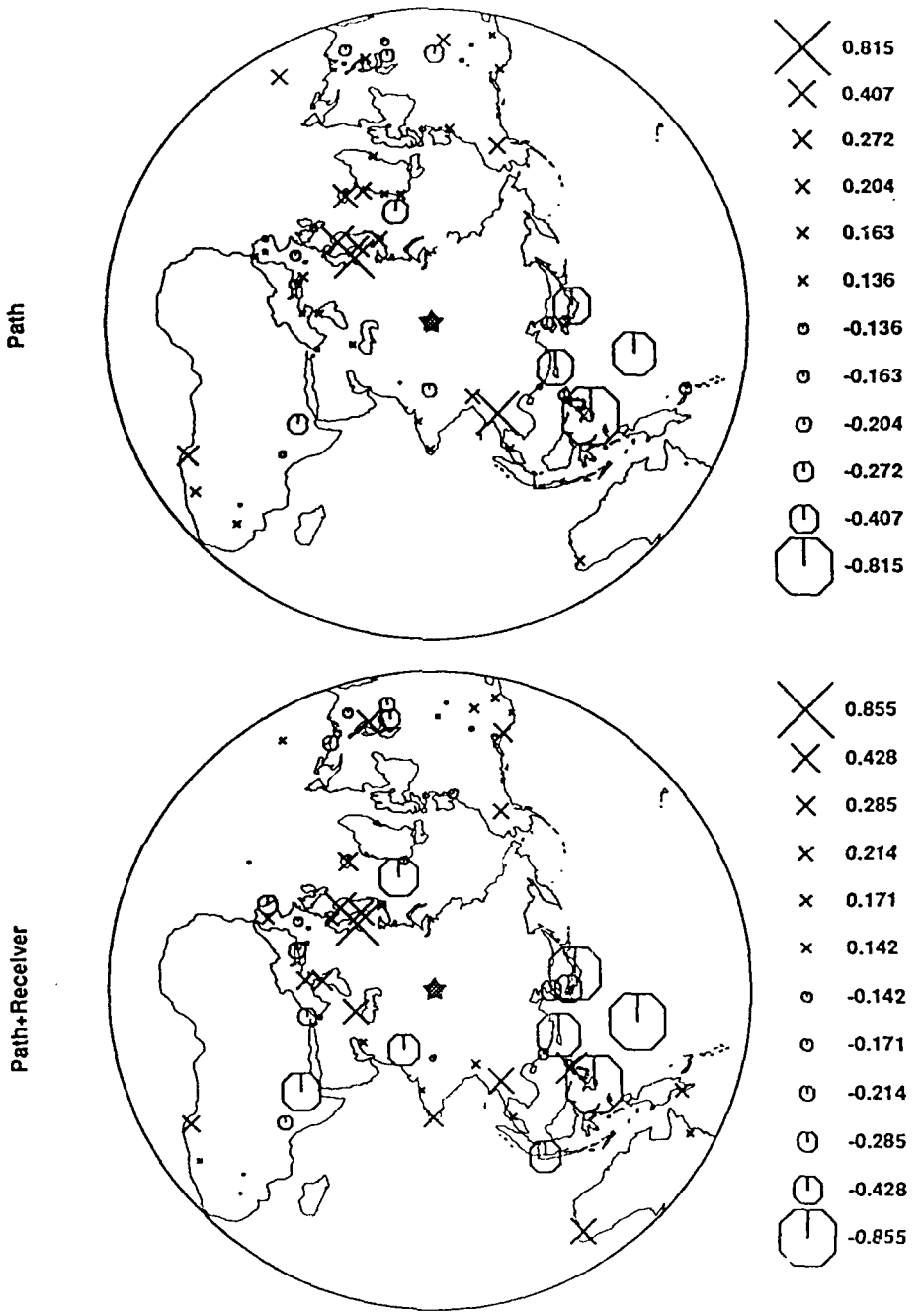

Figure 4. Same as Figure 3 except for the transition zone of Balapan test site.

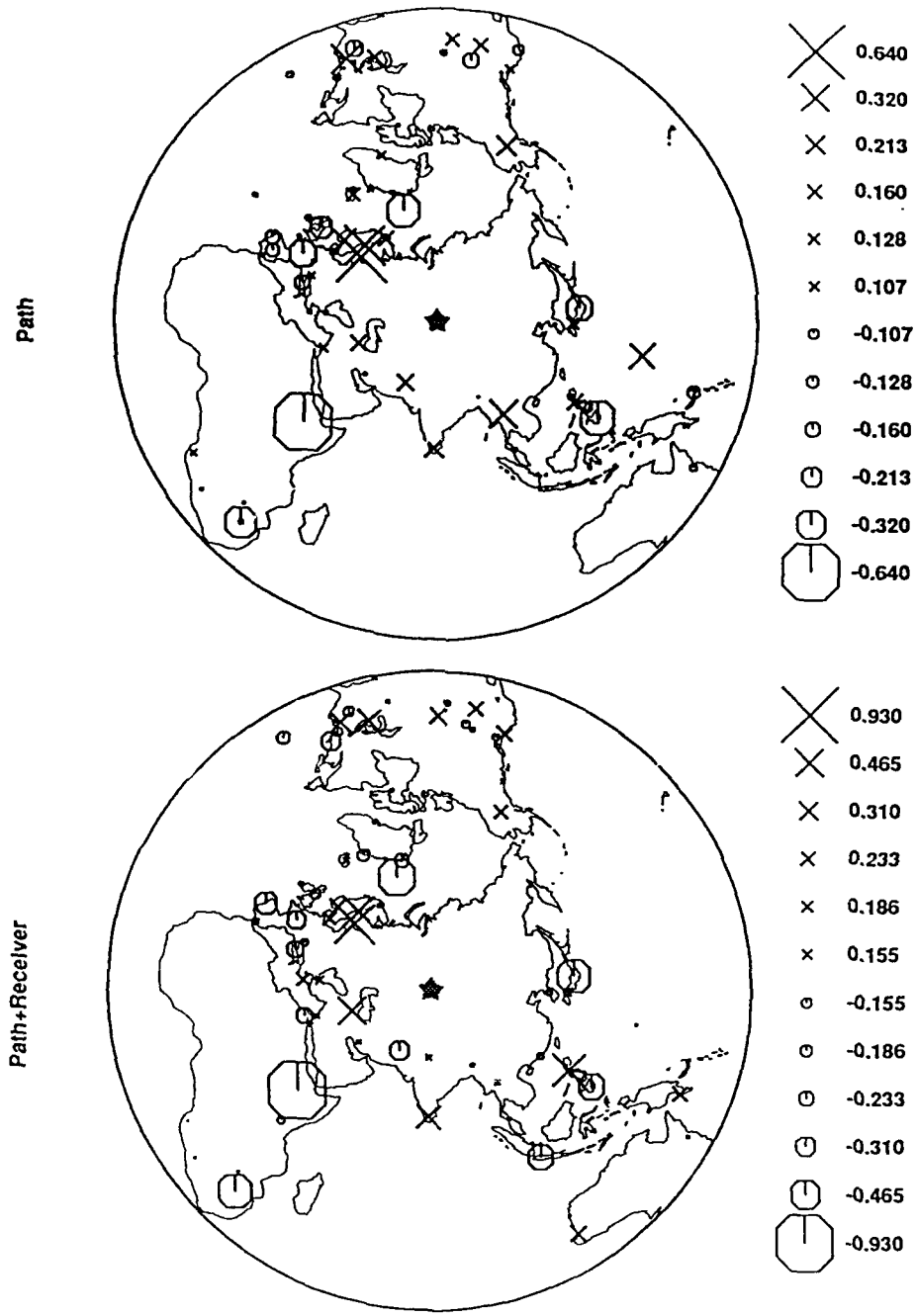

Figure 5. Same as Figure 3 except for the northeastern region of Balapan test site.

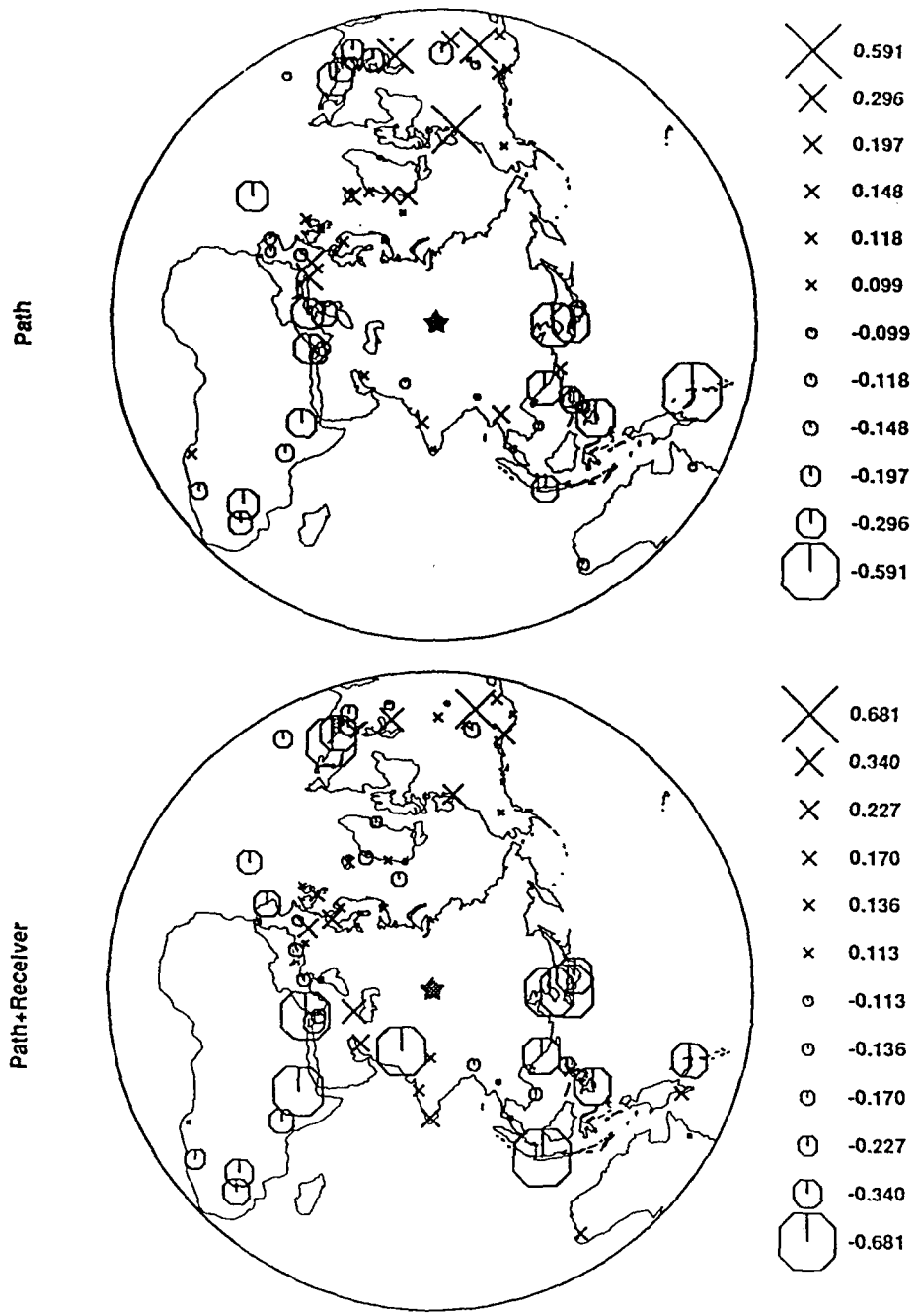

Figure 6. Same as Figure 3 except for Degelen test site.

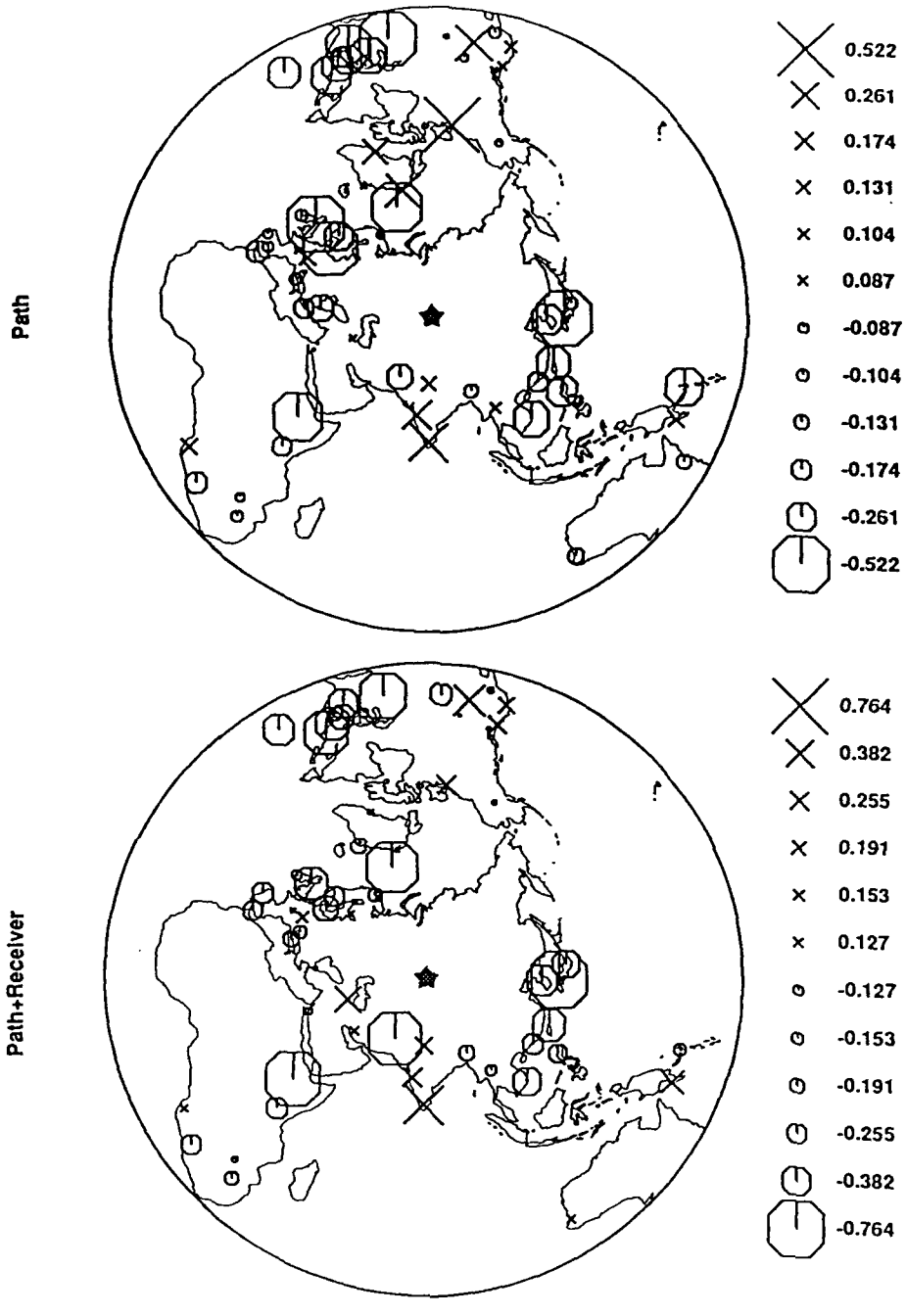

Figure 7. Same as Figure 3 except for Murzhik test site.

Table 2. Receiver and Path Effect on m_b of Semipalatinsk Events								
Station				Path Terms [F]				
Code	Lon	Lat	Rcv[1]	BSW	BTZ	BNE	Deg	Mzk
AAE	38.766	9.029	-0.290	-0.439	-0.274	-0.640	-0.287	-0.447
AAM	-83.656	42.300	0.210	0.267	0.140	0.163	-0.224	-0.335
AKU	-18.107	65.687	-0.053	0.169	0.342	0.155	0.185	0.043
ANP	121.517	25.183	-0.139	-0.232	-0.514	____	0.123	-0.301
AQU	13.403	42.354	-0.102	-0.167	-0.141	-0.159	-0.051	-0.104
ATU	23.717	37.972	0.171	0.050	-0.088	0.040	-0.312	-0.176
BAG	120.580	16.411	0.030	-0.189	-0.148	-0.064	-0.213	-0.273
BEC	-64.681	32.379	-0.120	0.160	0.216	-0.072	-0.087	-0.289
BKS	-122.235	37.877	0.104	-0.008	-0.015	-0.116	-0.026	0.112
BLA	-80.421	37.211	0.022	-0.165	-0.158	-0.184	-0.217	-0.410
BOZ	-111.633	45.600	0.046	____	-0.068	-0.166	0.055	-0.074
BUL	28.613	-20.143	-0.004	-0.112	0.047	-0.024	-0.312	-0.079
CHG	98.977	18.790	-0.234	0.268	0.623	0.319	0.177	0.097
CMC	-115.083	67.833	-0.270	____	0.134	____	0.512	0.522
COL	-147.793	64.900	-0.002	0.041	0.235	0.220	0.074	-0.067
COP	12.433	55.683	0.174	0.016	0.032	0.038	0.047	-0.499
COR	-123.303	44.586	0.161	0.030	0.127	0.096	0.095	0.086
CTA	146.254	-20.088	0.130	-0.096	-0.026	-0.074	-0.081	-0.130
DAG	-18.770	76.770	-0.076	0.218	0.100	0.047	0.169	____
DAV	125.575	7.088	-0.040	-0.457	-0.815	-0.377	-0.394	____
DUG	-112.813	40.195	0.074	0.220	0.056	0.159	0.390	0.350
EIL	34.950	29.550	-0.067	____	0.040	____	-0.176	-0.026
ESK	-3.205	55.317	0.084	0.002	-0.095	-0.240	0.085	-0.522
FLO	-90.370	38.802	-0.100	____	-0.110	____	-0.005	-0.518
FVM	-90.426	37.984	0.069	-0.023	-0.068	-0.004	-0.021	____
GDH	-53.533	69.250	-0.155	0.180	0.115	0.103	0.026	0.235
GEO	-77.067	38.900	-0.006	0.070	0.024	0.345	-0.043	-0.177

1) mean receiver bias that needs be corrected in addition to the path correction.

Table 2. Receiver and Path Effect on m_b of Semipalatinsk Events								
Station				Path Terms [F]				
Code	Lon	Lat	Rcv	BSW	BTZ	BNE	Deg	Mzk
GOL	-105.371	39.700	-0.237	0.164	0.187	0.144	0.181	-0.050
GSC	-116.805	35.302	0.022	0.058	0.095	0.011	0.106	-0.104
GUA	144.912	13.538	-0.232	0.069	-0.613	0.278	____	____
HKC	114.172	22.304	-0.087	0.015	-0.069	-0.017	-0.347	-0.179
HLW	31.342	29.858	-0.256	-0.077	0.006	0.004	-0.311	____
HNR	159.947	-9.432	0.220	-0.197	____	____	____	____
IST	28.996	41.046	0.184	0.122	0.111	-0.045	-0.255	-0.235
JER	35.197	31.772	-0.014	-0.060	-0.059	0.099	-0.148	-0.015
KBS	11.924	78.918	-0.227	-0.111	-0.341	-0.361	0.058	-0.457
KEV	27.007	69.755	-0.108	0.320	0.239	0.176	0.064	-0.064
KOD	77.467	10.233	0.177	0.280	0.119	0.213	0.045	0.364
KON	9.598	59.649	0.000	0.352	0.460	0.262	0.105	-0.260
KRK	30.062	69.724	0.069	____	____	____	0.030	0.044
KTG	-21.983	70.417	-0.254	0.132	0.241	0.064	0.099	0.055
LEM	107.617	-6.833	-0.417	0.046	-0.045	0.019	-0.264	____
LON	-121.810	46.750	-0.121	0.002	0.032	0.025	0.143	0.067
LOR	3.851	47.267	0.008	-0.244	-0.138	-0.295	-0.122	0.064
MAL	-4.411	36.728	-0.056	0.174	0.086	-0.041	-0.020	-0.193
MAN	121.077	14.662	0.367	____	0.098	0.175	-0.220	____
MAT	138.207	36.542	-0.256	-0.536	-0.528	-0.279	-0.166	-0.107
MDS	-89.760	43.372	-0.091	____	-0.188	____	0.371	____
MSO	-113.941	46.829	-0.091	-0.188	0.026	0.014	-0.087	____
MUN	116.208	-31.978	0.256	0.002	0.137	0.013	-0.108	-0.137
NAI	36.804	-1.274	-0.110	-0.019	-0.097	-0.004	-0.167	-0.168
NDI	77.217	28.683	0.100	-0.184	-0.188	0.001	0.008	0.134
NHA	109.212	12.210	-0.049	____	____	____	-0.096	-0.323
NOR	-16.683	81.600	-0.247	0.464	0.128	0.022	0.186	0.306

Table 2. Receiver and Path Effect on m_b of Semipalatinsk Events								
Station				Path Terms [F]				
Code	Lon	Lat	Rcv	BSW	BTZ	BNE	Deg	Mzk
NUR	24.651	60.509	0.089	0.421	0.557	0.564	-0.036	0.006
OGD	-74.596	41.088	-0.164	-0.068	0.060	0.024	-0.258	-0.282
PDA	-25.663	37.747	0.043	-0.065	0.005	-0.048	-0.316	____
PMG	147.154	-9.409	0.177	-0.036	0.030	0.058	-0.016	0.150
POO	73.850	18.533	-0.004	0.126	0.097	-0.016	0.131	0.266
PRE	28.190	-25.753	-0.074	0.033	0.103	0.051	-0.232	-0.100
PTO	-8.602	41.139	-0.193	-0.017	-0.081	-0.149	-0.121	-0.084
QUE	66.950	30.188	-0.484	0.090	0.029	0.182	-0.095	-0.226
RAB	152.170	-4.191	0.184	-0.258	-0.160	-0.137	-0.591	-0.341
RCD	-103.208	44.075	0.334	-0.016	-0.259	-0.066	-0.232	____
SCP	-77.865	40.795	-0.060	0.009	0.058	0.055	-0.131	-0.264
SDB	13.572	-14.926	-0.049	____	0.290	0.077	0.100	0.151
SEO	126.967	37.567	-0.125	-0.175	-0.167	0.025	-0.452	-0.279
SHI	52.520	29.638	0.120	-0.033	-0.017	-0.038	0.083	0.002
SHK	132.678	34.532	-0.250	-0.079	-0.148	0.135	-0.377	-0.514
SHL	91.883	25.567	-0.081	0.169	0.212	0.019	-0.056	-0.117
SLR	28.282	-25.735	-0.185	-0.268	____	-0.343	____	____
SNG	100.620	7.173	0.005	0.066	0.109	0.046	-0.063	0.008
STU	9.195	48.772	-0.001	0.030	0.049	-0.024	0.227	0.153
TAB	46.327	38.068	0.290	-0.074	0.085	0.170	-0.003	0.067
TOL	-4.049	39.881	0.120	-0.072	0.066	-0.139	-0.108	-0.095
TRI	13.764	45.709	-0.193	0.153	0.134	0.074	0.271	0.028
UME	20.237	63.815	0.070	0.634	0.302	0.454	-0.011	-0.007
VAL	-10.244	51.939	-0.024	0.050	0.002	-0.060	0.105	-0.105
WES	-71.322	42.385	-0.228	-0.058	0.013	-0.075	-0.352	-0.357
WIN	17.100	-22.567	-0.065	0.054	0.138	0.038	-0.161	-0.187

Marshall *et al.* (1992) analyze Degelen and Murzhik events recorded at 4 U.K.-designed arrays, and they find that EKA and GBA have distinguishable path effects for these two test sites. Amplitudes of Murzhik events are significantly reduced at EKA, whereas those of Degelen events are magnified. On the other hand, GBA shows a strong enhancement for Muzhik signals, but nearly no effect on Degelen events. At YKA or WRA, the station/path effects are about the same for Degelen and Murzhik explosions. All these observations (Figure 6 of Marshall *et al.*, 1992) are in excellent agreement with our result based on WWSSN recordings. The following is excerpted from Table 2, which illustrates the distinct path effects at EKA and GBA (see also Table 1 of Jih and Wagner, 1991b):

Table 3. Path Terms for Stations Close to EKA

Station	Test Site		Δ^*
Code	Degelen	Murzhik	(km)
ESK	0.085	-0.522	3.4
VAL	0.105	-0.105	602
KON	0.105	-0.260	903
COP	0.047	-0.499	985

*) Δ: distance from EKA.

Table 4. Path Terms for Stations Close to GBA

Station	Test Site		Δ^*
Code	Degelen	Murzhik	(km)
KOD	0.045	0.364	373
POO	0.131	0.266	666
NDI	0.008	0.134	1669

*) Δ: distance from GBA.

Note that the consistent trend across stations of wide spatial spread as illustrated in Tables 3 and 4 suggests that these path effects are due to some very near-source focusing/defoucusing feature.

To further illustrate the robustness of the proposed m_b determination scheme, Figures 8 through 15 show the raw and corrected m_b of 8 important explosions from Eastern Kazakhstan. Figure 8 shows the scatter plot of 3 different types of station m_bs for Soviet Joint Verification Experiment [JVE] explosion 880914B. The 25 good recordings and 1 clipped signal are shown with filled circles and upward arrow, respectively. The raw station m_bs (top) have a standard deviation of 0.19 m.u. Applying the "primary" station corrections (*i.e.*, the "Rcv" column in Table 2 or the "S" term in [3]) and the "secondary" corrections (*i.e.*, the "Path" column in Table 2 or "F" term in [3]) reduces the scatter down to 0.11 m.u. The dashed lines of 1 σ range around the network-averaged m_b clearly illustrate the remarkable reduction of fluctuation across the recording stations. The mean event m_b itself is not significantly changed, however.

Among the eight Semipalatinsk events shown here, the event 790804B (Figure 9) has the smallest scatter in the resulting $m_{2.9}$ values. The dramatic reduction of variation from m_1 to $m_{2.9}$ shows a factor of nearly 3, as compared to the worst case of about 2.11 for the event 811018B (Figure 12). Novaya Zemlya events typically exhibit a reduction factor around 2 (Jih and Wagner, 1992). Note that the path correction proposed in this study not only reduces the m_b scatter at stations that reported the good signals, but it also improves the data consistency of the censored recordings, as indicated by the shifting of the clipping recordings in Figure 9.

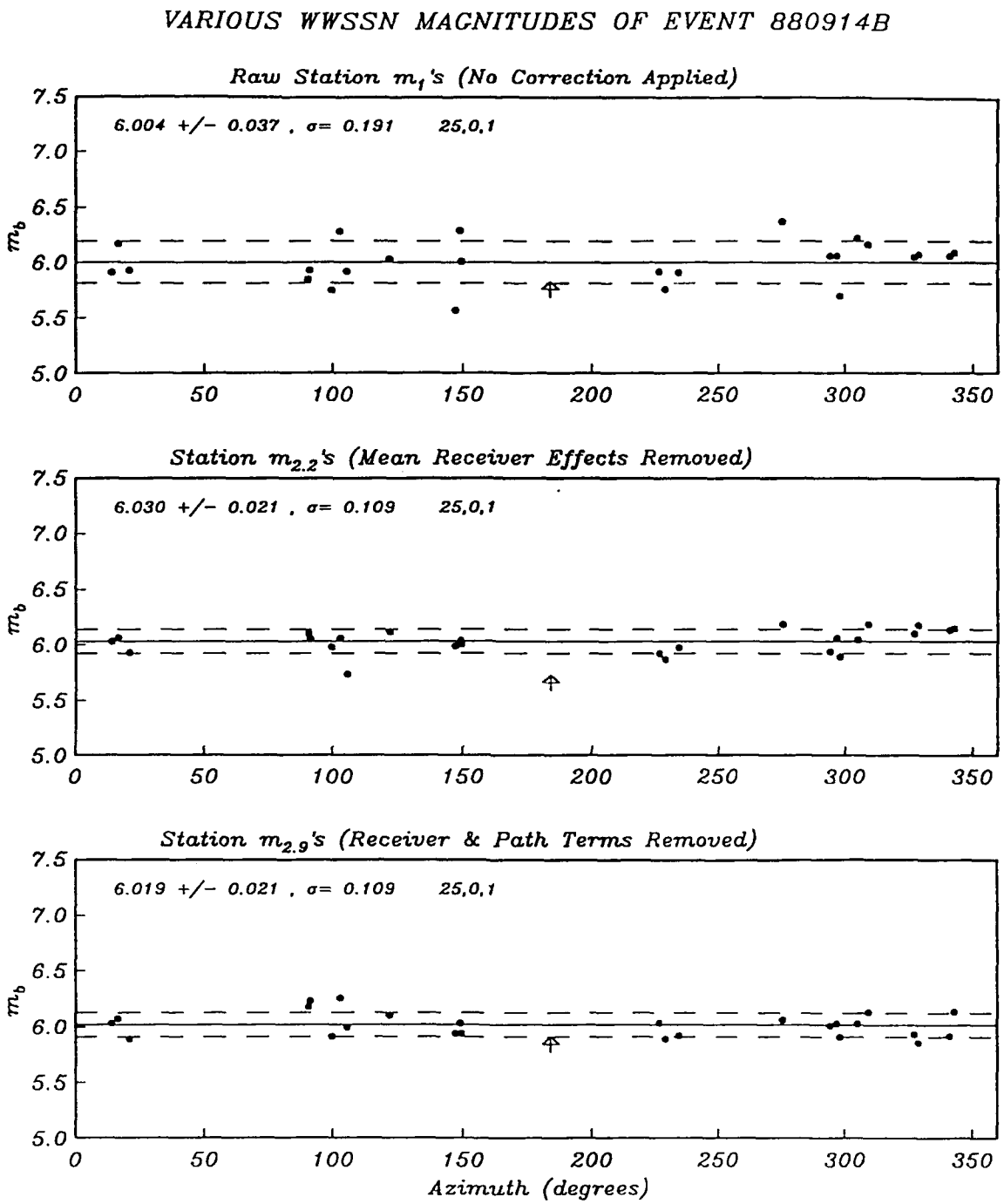

Figure 8. Scatter plot of 3 different types of station m_bs for Soviet JVE (880914B). The 25 good recordings and 1 clip are shown with filled circles and upward arrow, respectively. The raw station m_bs (top) have a standard deviation of 0.19 m.u. Applying the "primary" station corrections and the "secondary" path corrections reduces the scatter down to 0.11 m.u. (bottom). The dashed lines around the network-averaged m_b clearly illustrate the remarkable reduction of fluctuation across the recording stations. The mean event m_b itself is not significantly changed, however.

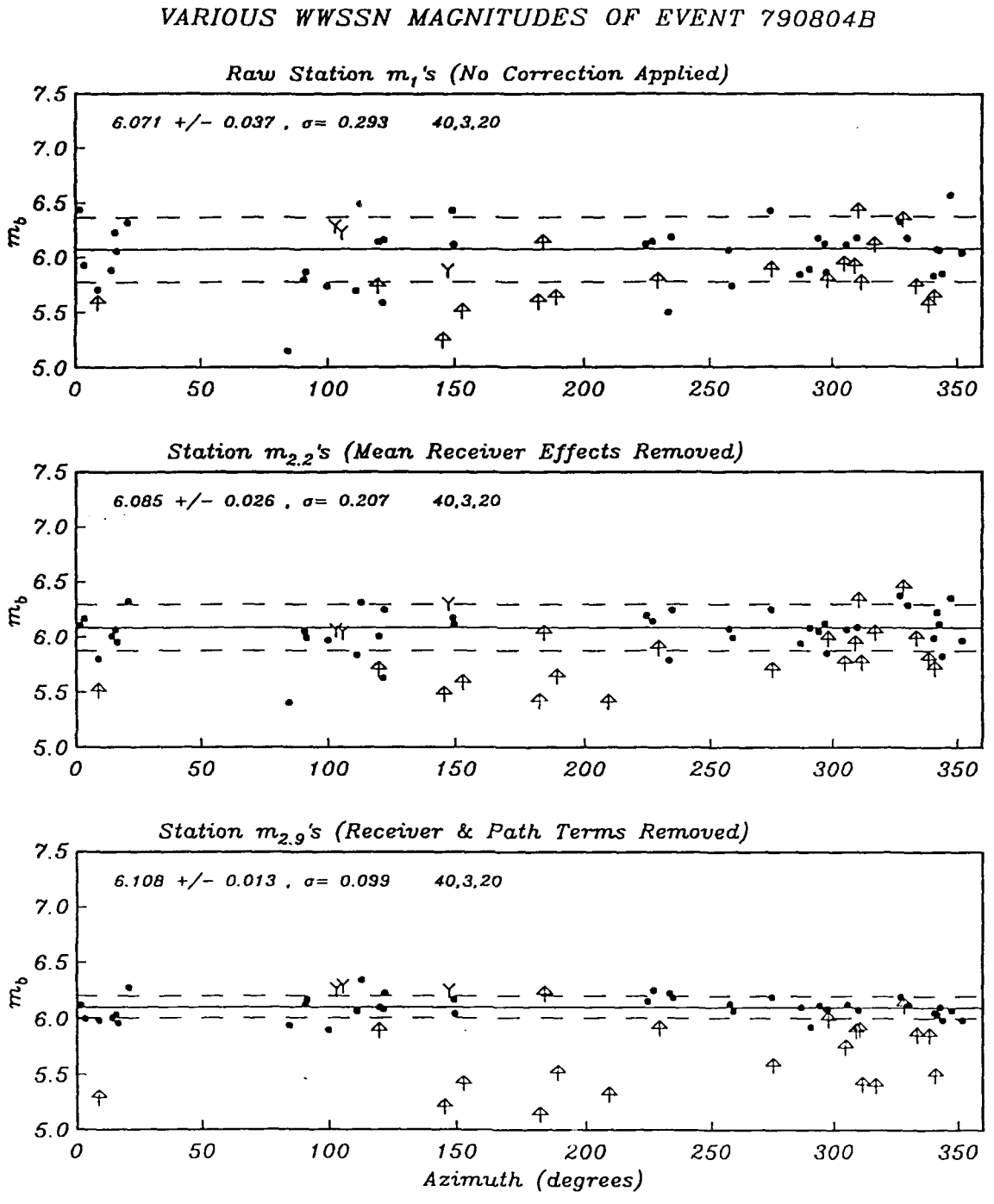

Figure 9. Scatter plot of 3 different types of station m_bs for the "historical" Balapan explosion 790804B. The three noise measurements are shown as downward arrows. This event has extremely small scatter in the resulting $m_{2.9}$ values. The dramatic reduction of variation from m_1 to $m_{2.9}$ shows a factor of nearly 2.97.

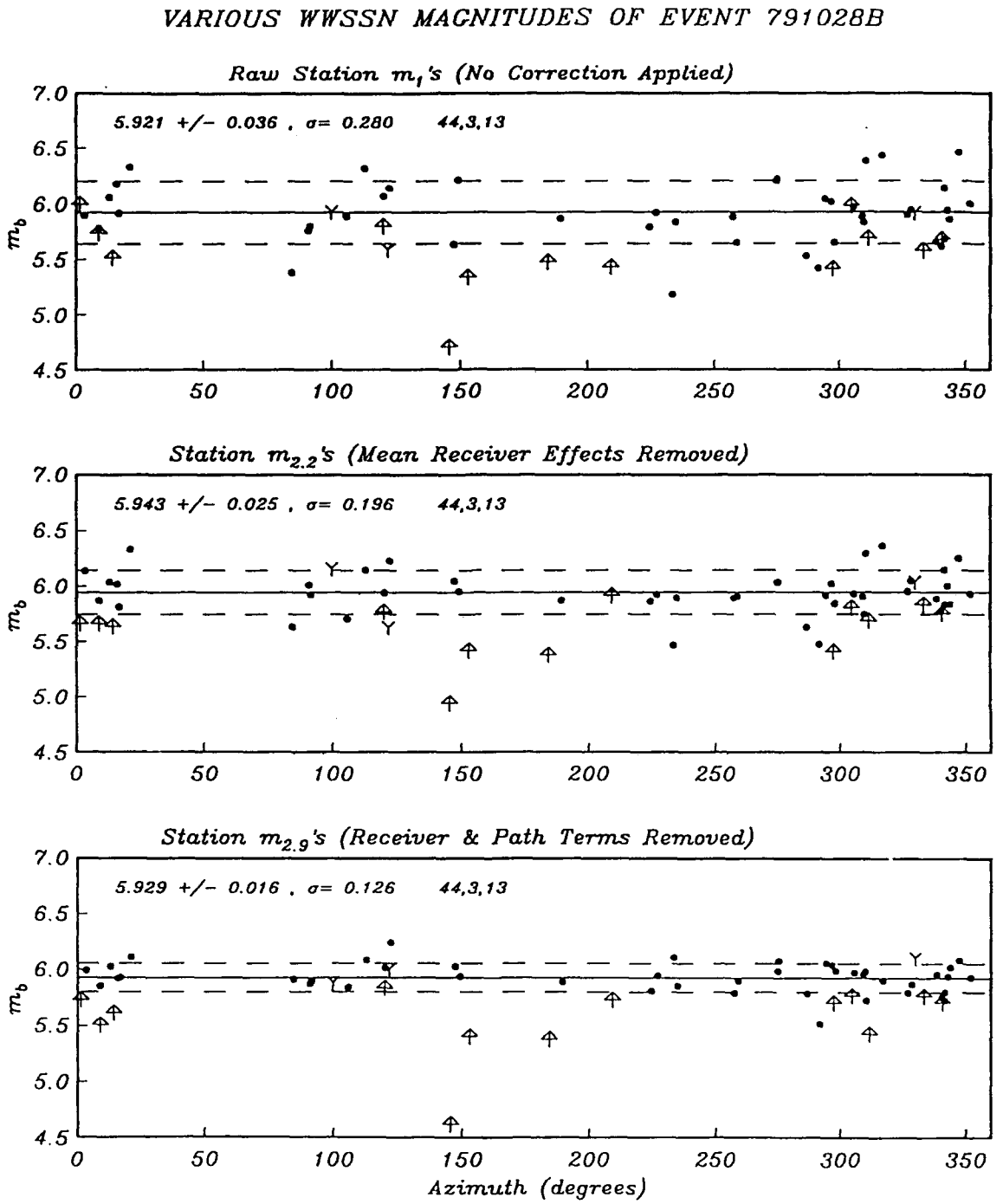

Figure 10. Scatter plot of 3 different types of station m_bs for the "historical" Balapan explosion 791028B.

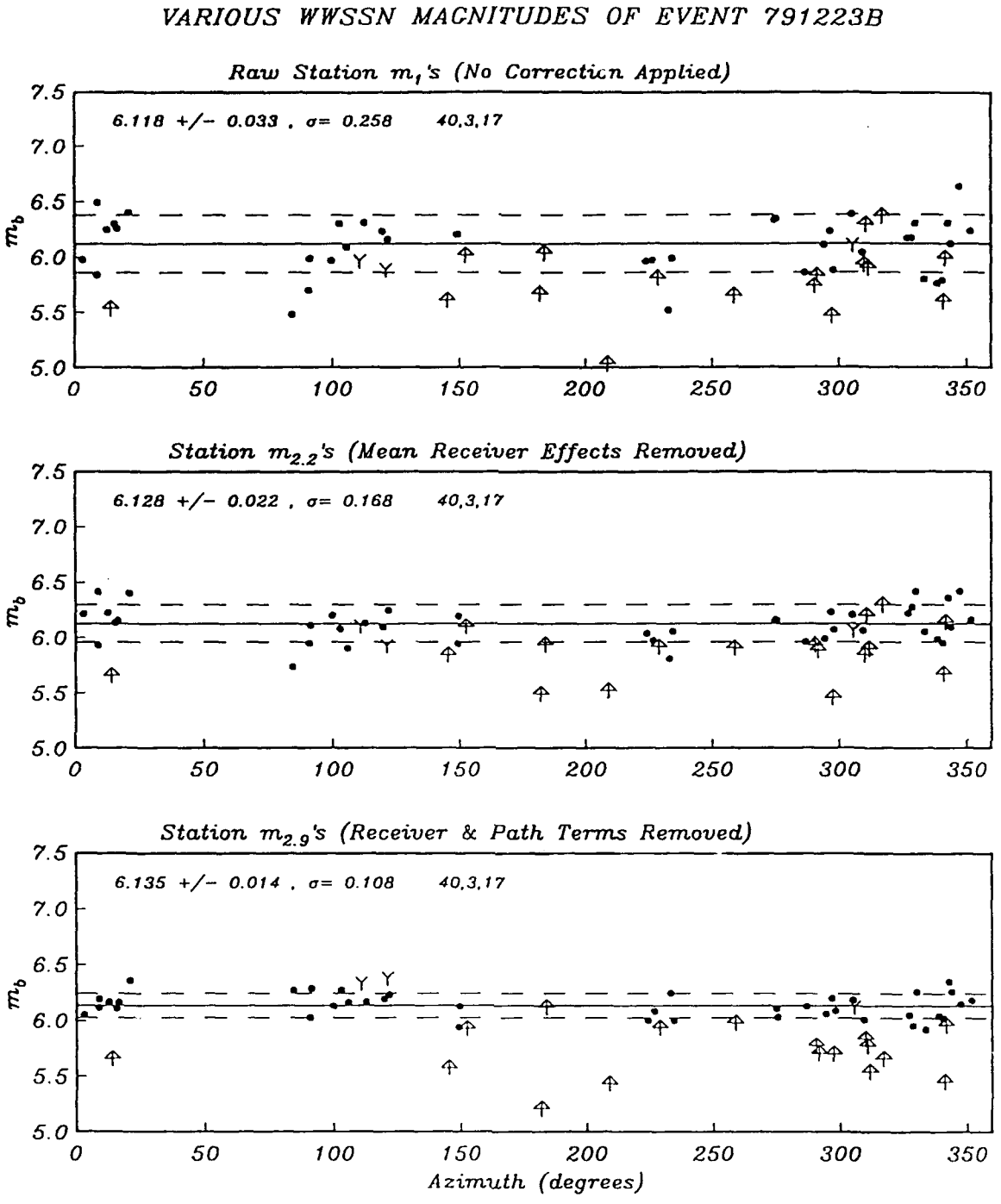

Figure 11. Scatter plot of 3 different types of station m_bs for the "historical" Balapan explosion 791223B.

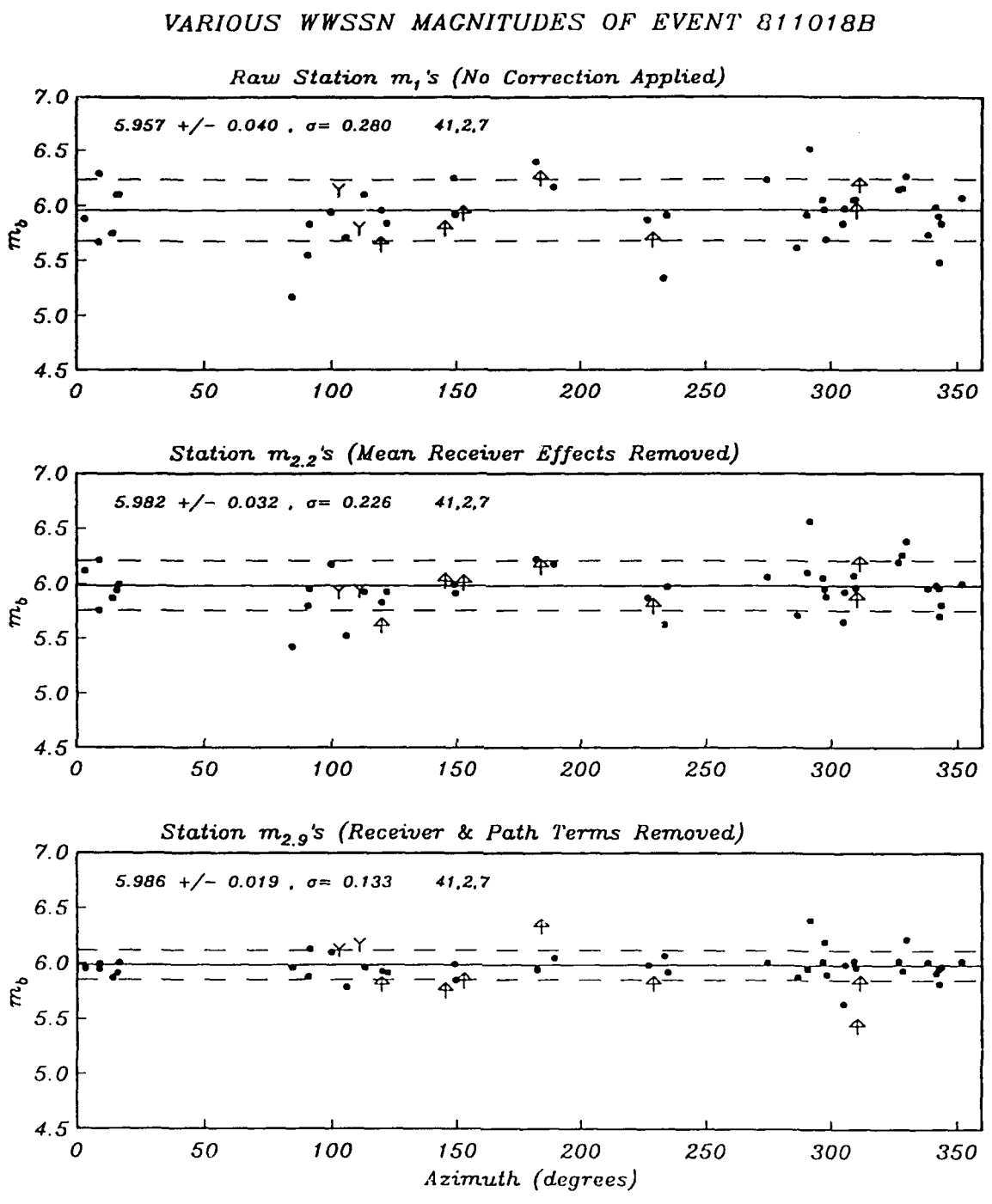

Figure 12. Scatter plot of 3 different types of station m_bs for the "historical" Balapan explosion 811018B.

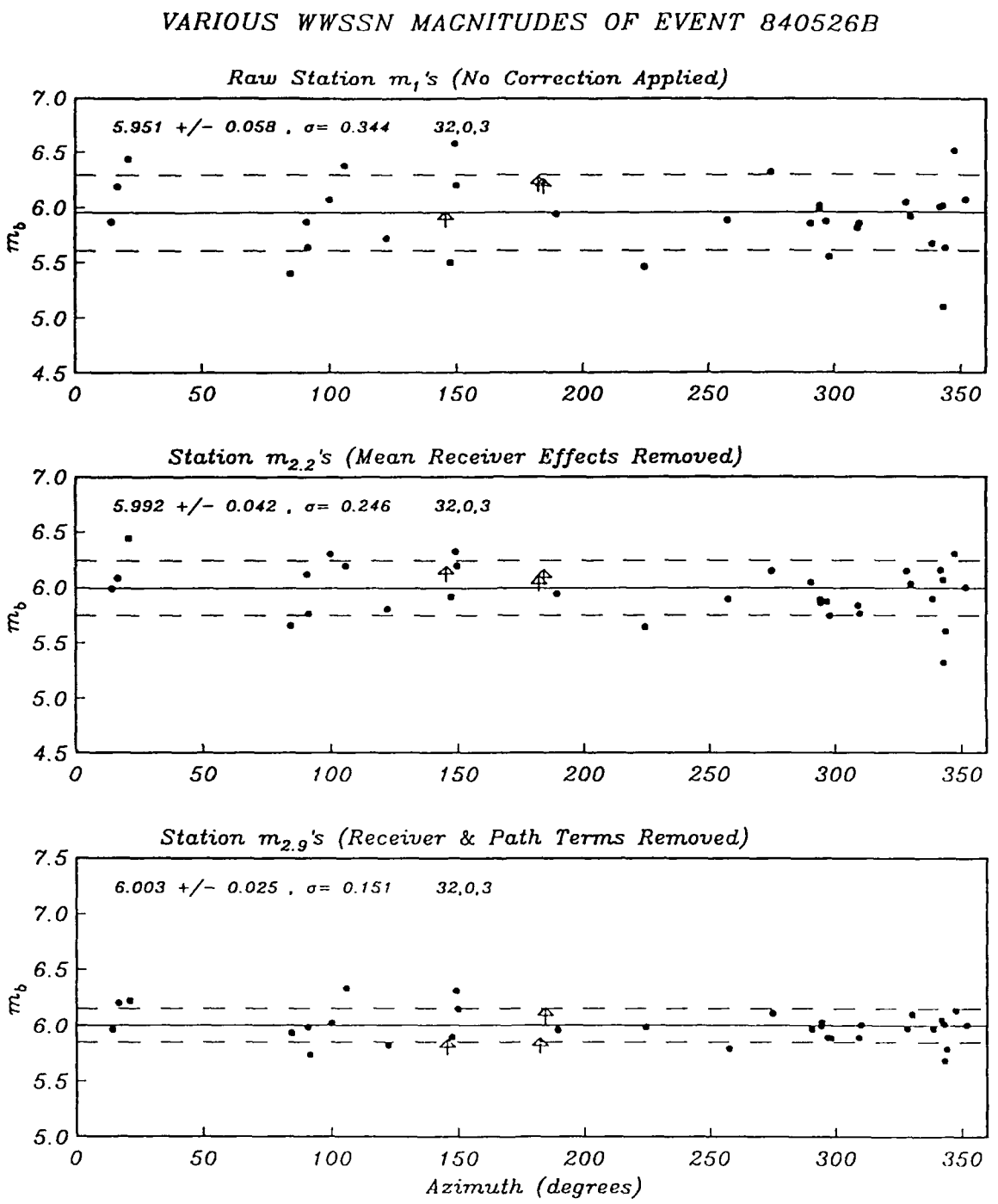

Figure 13. Scatter plot of 3 different types of station m_bs for the "historical" Balapan explosion 840526B.

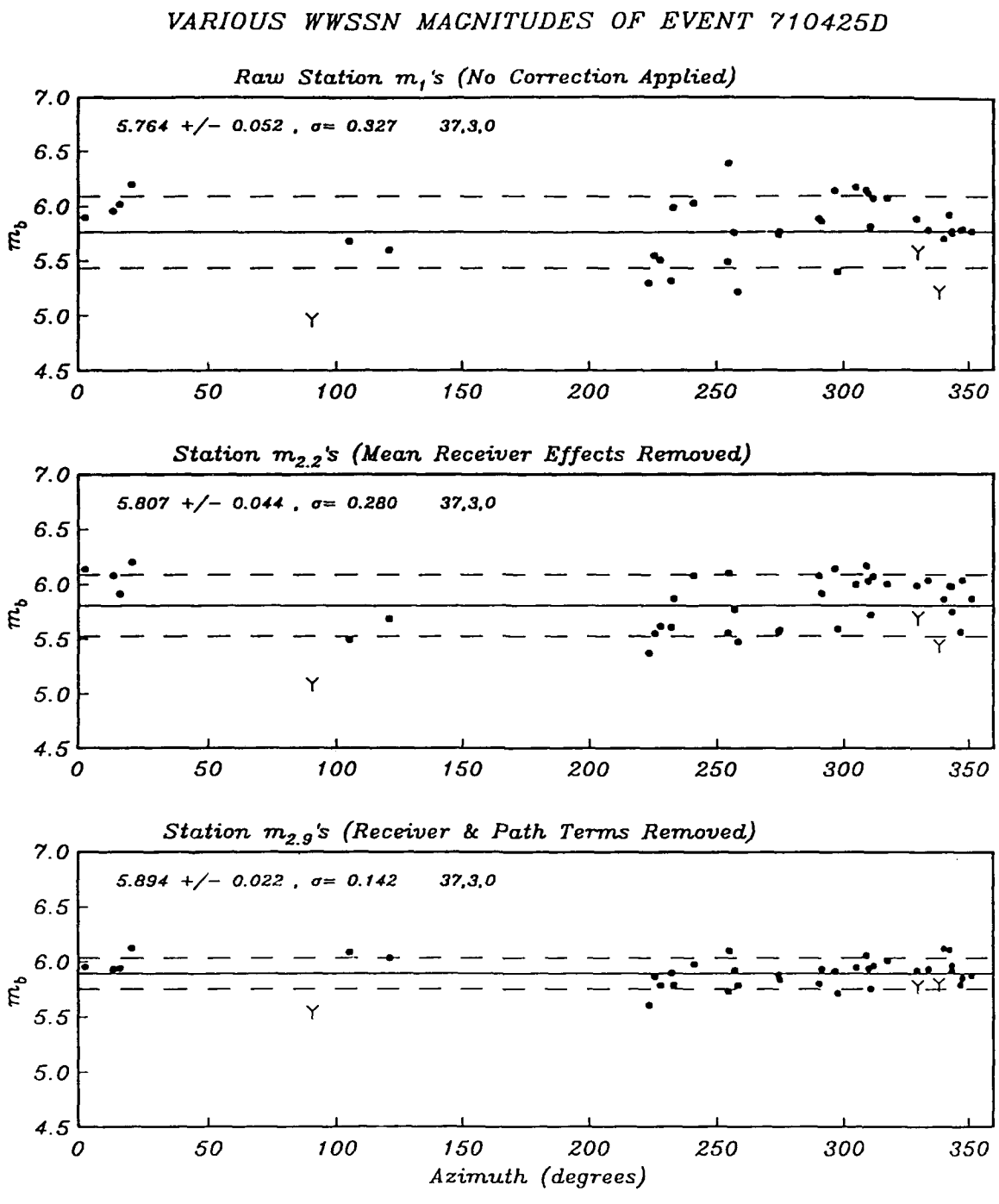

Figure 14. Scatter plot of 3 different types of station m_bs for Degelen explosion 710425D.

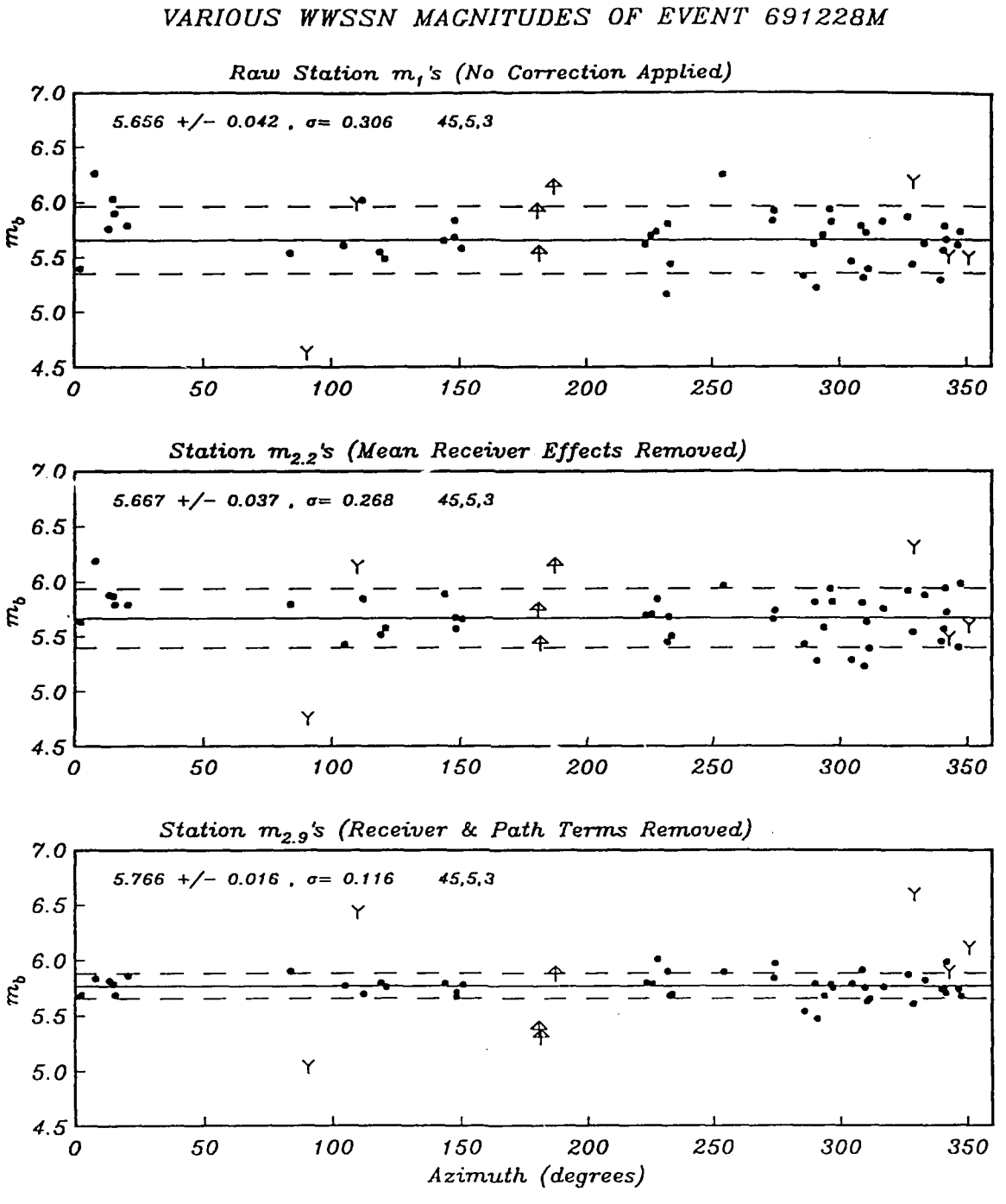

Figure 15. Scatter plot of 3 different types of station m_bs for Murzhik explosions 691223M.

4. YIELD ESTIMATES OF SEMIPALATINSK EXPLOSIONS

It is fortuitous to have the source information released by Bocharov *et al.* (1989) (and Vergino, 1989) to calibrate the Semipalatinsk test site. The small scatter around the following calibration curves based on the regression of our path-corrected m_b on the published yields illustrates how well the fit can be at the Central Asian test site.

$$m_b(P_a) = 0.802(\pm 0.020)\ \log(W) + 3.834(\pm 0.032) \quad [6]$$

$$m_b(P_b) = 0.800(\pm 0.020)\ \log(W) + 4.130(\pm 0.031) \quad [7]$$

$$m_b(P_{max}) = 0.768(\pm 0.019)\ \log(W) + 4.399(\pm 0.030) \quad [8]$$

Figures 16 through 18 show the regression of $\overline{m}_{2.9}(P_a)$, $\overline{m}_{2.9}(P_b)$, and $\overline{m}_{2.9}(P_{max})$ on the the Soviet yields published by Bocharov *et al.* (1989), which correspond to Equations [6] through [8], respectively. The uncertainties in the m_bs and the yields are taken into account through 800 bootstrap resamplings. The darkened bundle is actually the collection of all 800 regressions, each produced by a possible realization of 11 perturbed (m_b, yield) pairs. The 95% confidence band (shown as 2 curves around the darkened bundle) is narrower near the centroid and wider towards both ends, as expected. The individual 95% confidence intervals of the two inferred parameters (*i.e.*, the slope and the intercept of the calibration curve) are shown with the dashed line in the scatter plot (bottom). Note that the dashed rectangle is not the joint 90% confidence interval, however, due to the highly correlated nature of the two parameters. Degelen event 660507D is not included in these regressions, as suggested by Jih and Wagner (1991b).

We have utilized these calibration curves to estimate the yield of all 92 Semipalatinsk explosions in our data set, and the result is summarized in Table 5. For cratering events (such as 650115B) the yield estimate based on the first motion (*i.e.*, P_a) should be used, since no depth correction (*e.g.*, Marshall *et al.*, 1979) has been applied to $m_b(P_b)$ or $m_b(P_{max})$ in Table 5. For this particular event, Myasnikov *et al.* (1970) gave a "scaled apparent radius" and scaled depth of of 51 and 50 m/KT$^{0.33}$, respectively. Combining this information with the crater radius and the emplacement depth released at the IAEA symposium, Ringdal and Marshall (1989) inferred the yield of this explosion as 111 KT, which is identical to our estimate based on P_a (Table 5). This example illustrates that P_a from hard-rock test sites in stable region could be a very favorable phase for the source size determination.

Much of the source information about the Soviet JVE explosion (880914B, Figure 8) has not been released. The *"New York Times"* (Gordan, 1988) states that the American and Soviet on-site measurements are said to give yields of 115 KT and 122 KT, respectively. If we substitute the $\overline{m}_{2.9}(P_a)$ of JVE into Equation [6], the mean yield estimate would be 113 KT with a 95%-uncertainty factor of 2.2 (*cf.* Figure 16). If the averaged on-site measurement of 119 KT was accurate, then our central-value estimate of 113 KT based on *P*-wave observations alone is off by 5% only.

The Soviet JVE has a *RMS* L_g measured at NORSAR of 5.969±0.01 (Ringdal and Marshall, 1989). Along with the other 8 *RMS* L_g values in Ringdal (1990), DWLSQ-derived calibration curve would give an estimate of 103 KT for JVE with a 95%-factor of 1.8., assuming a 10% standard error in the yields (Figure 14 of Jih and Wagner, 1991b). This yield estimate is nearly identical to the one obtained with the in-country regional network recordings. The *RMS* L_g of 5.980±0.02 (Israelson, 1991) corresponds to 100 KT and a 95%-factor of 1.9 based on either DWLSQ of Jih *et al.* (1991) or Ericsson's algorithm. In addition to the yield estimates cited above, Sykes and Ekstrom (1989) gave an estimate of 113 KT based on the arithmetic average of m_b and M_S. Priestley *et al.* (1990) analyzed the L_g amplitudes at 4 seismographs near the Semipalatinsk test range: KSU (Karasu), KKL (Karkaralinsk), BAY (Bayanual), and TLG (Talgar), and they obtained a $m_b(L_g)$ of 5.968±0.02. Murphy *et al.* (1991) gave a network-averaged m_b of 6.012 with a standard deviation of 0.190 across the network. They also derived a *RMS* L_g of 5.969 using 8 stations in U.S.S.R., Norway, and Manchuria. It is worth noting that all these seismic magnitudes give very consistent yield estimate in the range 100-150 KT, as specified in the bilateral agreement signed by U.S. and Soviet governments before JVE (Richards, 1990; Stump, 1991).

There are 15 events in common in Israelson's (1991) *RMS* L_g and our $\overline{m}_{2.9}$ data sets for which the Soviet-published yields are available, which yield a very weak correlation between the *RMS* L_g and $\overline{m}_{2.9}$ residuals (relative to the expected magnitude at the associated yield value) (Figure 19), and hence the combination of these two methods for better yield estimate is justifiable.

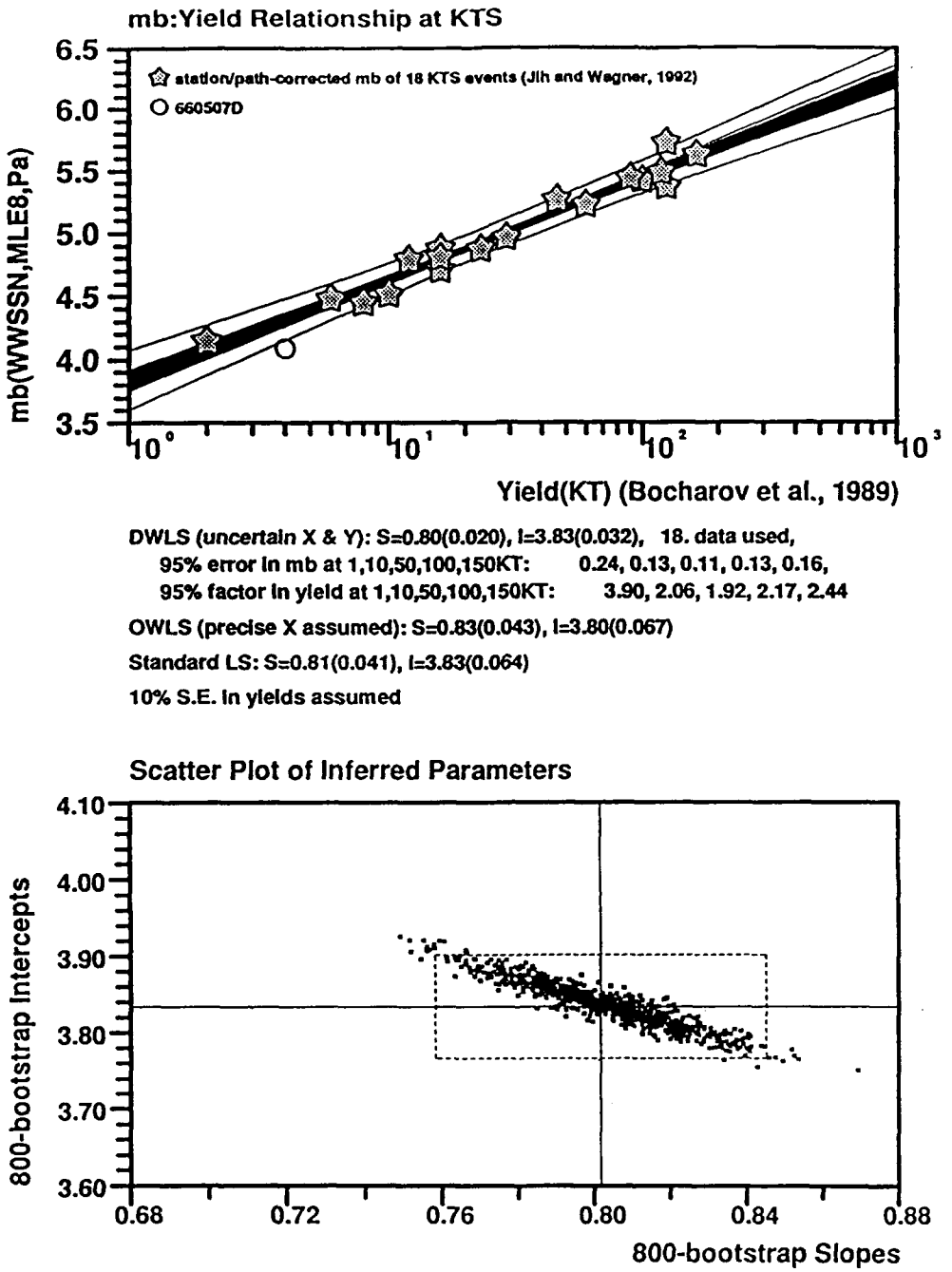

Figure 16. Regressing the $m_b(P_a)$ on 19 Soviet-published yields. The yields are assumed to be subject to 10% standard errors. The uncertainties in the m_bs and the yields are taken into account through 800 Monte-Carlo resamplings. The darkened bundle is actually the collection of all 800 regressions, each associated with a possible realization of 19 perturbed (m_b, yield) pairs. The 95% confidence band (shown as 2 curves around the darkened bundle) is most narrow near the centroid and wider towards both ends, as expected. The individual 95% confidence intervals of the two inferred parameters (*i.e.*, the slope and the intercept of the calibration curve) are shown with the dashed line in the scatter plot (bottom). Note that the dashed rectangle is not the joint 90% confidence interval, however, due to the highly correlated nature of the two parameters.

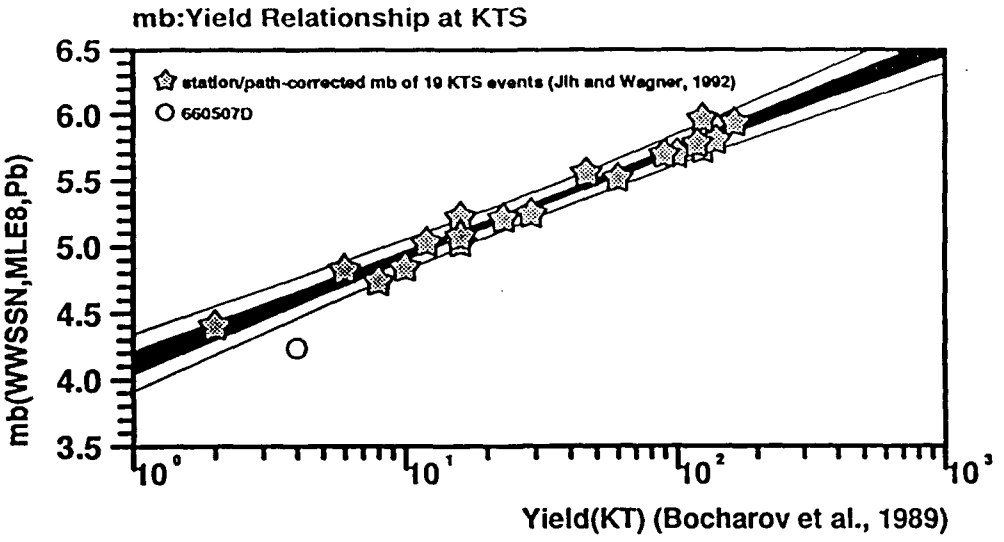

DWLS (uncertain X & Y): S=0.80(0.020), I=4.13(0.031), 19. data used,
95% error in mb at 1,10,50,100,150KT: 0.22, 0.12, 0.10, 0.12, 0.13,
95% factor in yield at 1,10,50,100,150KT: 3.45, 2.01, 1.81, 2.02, 2.17

OWLS (precise X assumed): S=0.82(0.035), I=4.10(0.055)

Standard LS: S=0.80(0.032), I=4.12(0.052)

10% S.E. in yields assumed

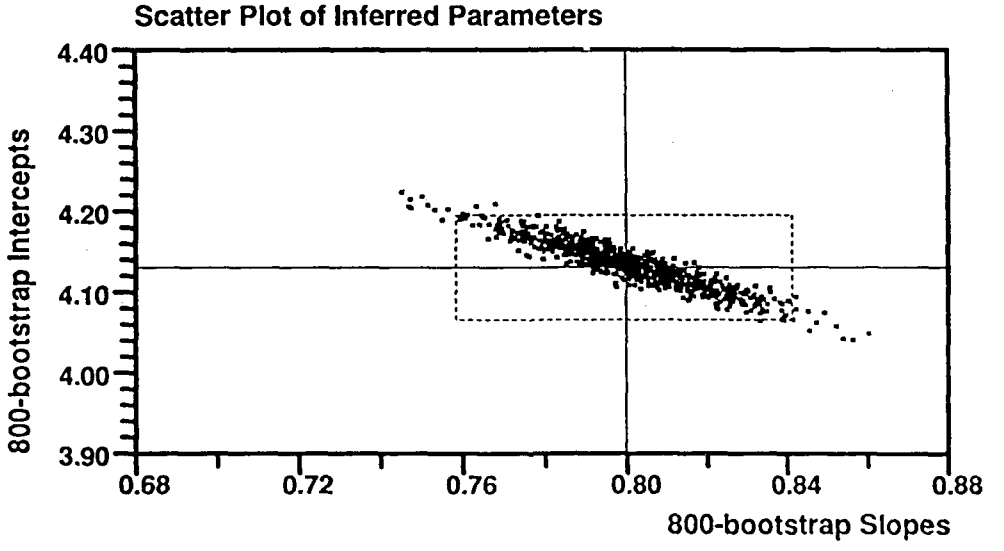

95% confidence interval of slope: 0.80+/-0.041
95% confidence interval of intercept: 4.13+/-0.065
[97.5% quantile of t(17. D.o.F.), 2.110, used]

Figure 17. Same as Figure 16 except for $m_b(P_b)$.

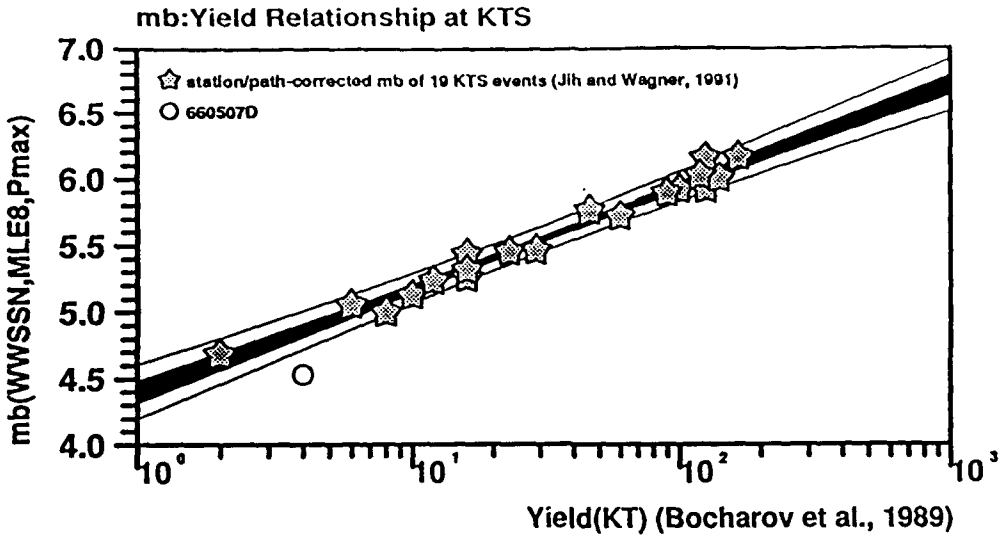

DWLS (uncertain X & Y): S=0.77(0.019), I=4.40(0.030), 19. data used,
95% error in mb at 1,10,50,100,150KT: 0.20, 0.12, 0.10, 0.12, 0.13,
95% factor in yield at 1,10,50,100,150KT: 3.39, 2.01, 1.81, 2.02, 2.17

OWLS (precise X assumed): S=0.78(0.032), I=4.38(0.051)

Standard LS: S=0.77(0.030), I=4.39(0.048)

10% S.E. in yields assumed

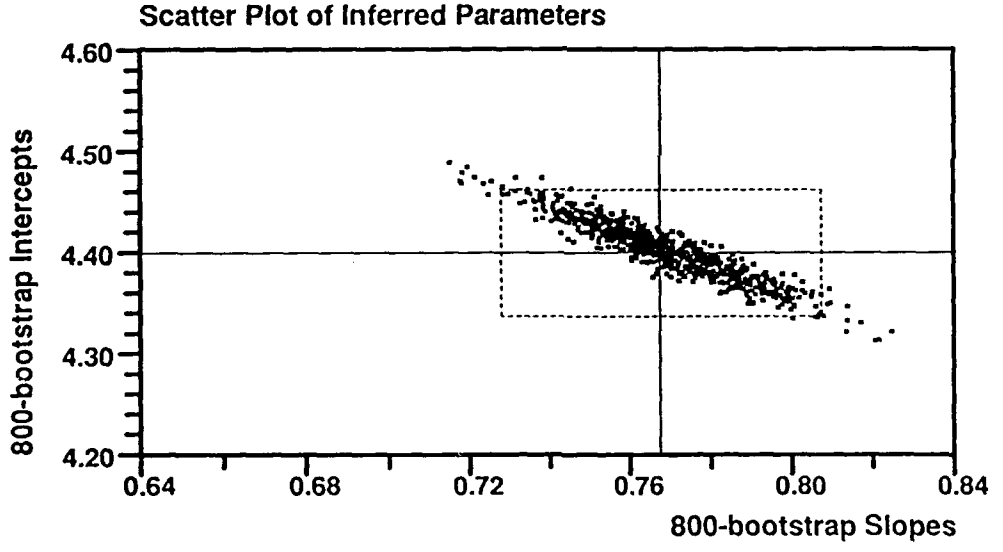

95% confidence interval of slope: 0.77+/-0.040
95% confidence interval of intercept: 4.40+/-0.063
[97.5% quantile of t(17. D.o.F.), 2.110, used]

Figure 18. Same as Figure 16 except for $m_b(P_{max})$.

Table 5. Yield Estimates of Semipalatinsk Explosions							
Event		Epicenter		Yield Estimate			Yield
Date	Site	Lon	Lat	P_a	P_b	P_{max}	Announced
650115B	BTZ	79.009	49.935	111	94	81	100-150
651121D	Deg	78.064	49.819	25	24	24	29
660213D	Deg	78.121	49.809	223	197	192	125
660320D	Deg	78.024	49.762	94	91	94	100
660507D	Deg	78.105	49.743	2	1	1	4
661019D	Deg	78.021	49.747	46	41	36	20-150
661218M	Mzk	77.747	49.925	88	75	78	20-150
670226D	Deg	78.082	49.746	100	89	94	20-150
670916M	Mzk	77.728	49.937	11	10	10	<20
670922M	Mzk	77.691	49.960	7	8	9	10
671122M	Mzk	77.687	49.942	—	1	1	<20
680619B	BNE	78.986	49.980	11	12	13	<20
680929D	Deg	78.122	49.812	54	53	51	60
690531M	Mzk	77.694	49.950	6	9	9	<20
690723D	Deg	78.130	49.816	12	13	13	16
690911D	Deg	77.997	49.776	2	2	3	<20
691130B	BTZ	78.956	49.924	80	101	94	125
691228M	Mzk	77.714	49.937	61	60	58	46
700721M	Mzk	77.673	49.952	12	13	14	<20
701104M	Mzk	77.762	49.989	24	18	17	<20
710322D	Deg	78.109	49.798	40	40	35	20-150
710425D	Deg	78.034	49.769	99	91	88	90
710606M	Mzk	77.660	49.975	20	23	22	16

Table 5. Yield Estimates of Semipalatinsk Explosions (continued)							
Event		Epicenter		Yield Estimate			Yield
Date	Site	Lon	Lat	P_a	P_b	P_{max}	Announced
710619M	Mzk	77.641	49.969	19	19	20	<20
710630B	BTZ	78.980	49.946	6	6	7	<20
711009M	Mzk	77.641	49.978	16	13	12	12
711021M	Mzk	77.597	49.974	20	22	23	23
711230D	Deg	78.037	49.760	36	42	38	20-150
720210B	BNE	78.878	50.024	17	15	15	16
720328D	Deg	78.076	49.733	6	7	7	6
720816D	Deg	78.059	49.765	6	6	6	8
720826M	Mzk	77.717	49.982	12	13	13	<20
720902M	Mzk	77.641	49.959	2	2	2	2
721102B	BSW	78.817	49.927	168	180	195	165
721210D	Deg	78.058	49.819	35	39	39	20-150
721210B	BNE	78.996	50.027	___	123	121	140
730723B	BTZ	78.850	49.980	240	208	203	___
731214B	BNE	79.010	50.040	58	59	59	___
750427B	BNE	78.980	49.990	22	24	29	___
760704B	BTZ	78.950	49.910	50	59	69	___
761123B	BNE	79.000	49.990	___	___	47	___
761207B	BSW	78.900	49.880	23	34	35	___
770329D	Deg	78.140	49.790	5	7	8	___
770730D	Deg	78.160	49.770	4	5	5	___
780326D	Deg	78.070	49.730	28	29	30	___
780422D	Deg	78.170	49.720	8	7	7	___

Table 5. Yield Estimates of Semipalatinsk Explosions (continued)							
Event		Epicenter		Yield Estimate			Yield
Date	Site	Lon	Lat	P_a	P_b	P_{max}	Announced
780611B	BSW	78.838	49.879	58	54	69	—
780705B	BSW	78.871	49.887	53	50	55	—
780728D	Deg	78.140	49.756	35	35	34	—
780829B	BNE	78.990	50.000	—	—	97	—
780915B	BTZ	78.940	49.910	93	81	73	—
781104B	BNE	78.943	50.034	39	33	33	—
781129B	BSW	78.760	49.950	—	—	86	—
790623B	BTZ	78.910	49.910	178	153	156	—
790707B	BNE	79.060	50.050	—	—	69	—
790804B	BSW	78.904	49.894	163	160	171	HE
790818B	BNE	79.010	49.970	—	—	162	—
791028B	BNE	78.997	49.973	107	92	99	HE
791202B	BSW	78.840	49.890	—	—	90	—
791223B	BSW	78.755	49.916	159	158	184	HE
800522D	Deg	78.082	49.784	13	12	11	—
800629B	BSW	78.815	49.939	51	45	44	—
800914B	BTZ	78.880	49.970	117	131	158	—
801012B	BNE	79.080	49.950	—	—	79	—
801214B	BTZ	79.000	49.930	—	—	95	—
801227B	BNE	79.040	50.040	—	—	90	—
810422B	BSW	78.900	49.900	—	—	96	—
810913B	BTZ	78.980	49.890	—	—	153	—
811018B	BSW	78.859	49.923	117	115	118	HE

Table 5. Yield Estimates of Semipalatinsk Explosions (continued)							
Event		Epicenter		Yield Estimate			Yield
Date	Site	Lon	Lat	P_a	P_b	P_{max}	Announced
811129B	BSW	78.860	49.887	32	30	29	—
811227B	BSW	78.870	49.900	—	—	219	—
820425B	BTZ	78.930	49.880	—	—	111	—
820704B	BTZ	78.850	49.990	—	—	143	—
820831B	BSW	78.761	49.924	8	8	8	—
821205B	BSW	78.840	49.910	—	—	168	—
821226B	BNE	78.988	50.071	46	36	37	—
830612B	BTZ	78.980	49.910	—	—	102	—
831006B	BSW	78.840	49.930	—	—	101	—
831026B	BTZ	78.910	49.920	—	—	118	—
831120B	BNE	78.999	50.047	23	18	17	—
840425B	BTZ	78.940	49.950	—	—	89	—
840526B	BNE	79.006	49.969	137	140	123	HE
840714B	BTZ	78.960	49.890	—	—	144	—
841027B	BSW	78.830	49.950	—	—	244	—
841202B	BNE	79.070	49.990	—	—	51	—
841216B	BTZ	78.860	49.960	—	—	136	—
841228B	BSW	78.750	49.860	—	—	97	—
850210B	BSW	78.781	49.888	69	66	74	—
850615B	BSW	78.880	49.890	—	—	145	—
850630B	BSW	78.658	49.848	91	86	89	—
870620B	BSW	78.740	49.927	127	111	121	—
880914B	BSW	78.808	49.833	113	114	129	JVE

5. MISCELLANEOUS COMPARATIVE STUDIES WITH m_b

In the initial attempt of Jih and Wagner (1991b) to correct for the path effects of Semipalatinsk explosions with "all three" subregions of Balapan test site treated as geologically and geophysically homogeneous, they reported that 3 out of 82 Semipalatinsk explosions appear anomalous in that $\overline{m}_{2.9}$ do not show significant reduction in the fluctuational variation across the recording network. The Soviet JVE explosion was one of the three anomalous events. It turns out that separating Balapan test site into three regions as suggested in Ringdal and Marshall (1989) (and Marshall *et al.*, 1984; Ringdal and Fyen, 1988) improves the performance significantly, and none of the three events would seem anomalous. Such partitioning of a test site according to the geophysical characteristics within a test site can provide very accurate yield estimate, as evidenced by our yield estimation exercise using P_a and P_b (*cf.* pages 34-35).

Tables 6 and 7 compare P_{max} and P_b relative to P_a at several Central Asian nuclear test sites. Note that there appears to be a bias of 0.11 m.u. in $m_b(P_{max})-m_b(P_a)$ between Eastern Kazakh and Novaya Zemlya. This bias could be largely due to the difference in *pP* interference at these two test sites, however (Jih and Wagner, 1992).

Table 6. $\overline{m}_{2.9}$(ML8), $m_b(P_{max})$ and $m_b(P_b)$ vs. $m_b(P_a)$

Site[1]	$m_b(P_b)-m_b(P_a)$	$m_b(P_{max})-m_b(P_a)$	#[2]
BSW	0.288±0.013	0.523±0.014	13
BTZ	0.289±0.033	0.516±0.059	4
BNE	0.236±0.020	0.445±0.013	5
Deg	0.317±0.027	0.557±0.037	6
KTS	0.285±0.010	0.515±0.013	28
NNZ	0.224±0.012	0.402±0.014	17
PRC	0.099±0.051	0.294±0.073	9

1) BSW = SW subsite, Balapan; BNE = NE subsite, Balapan; BTZ = transition zone, Balapan; Deg = Degelen Mountain; Mzk = Murzhik; KTS = all 5 subsites in Eastern Kazakh combined; NNZ = northern subsite, Novaya Zemlya; PRC = Lop Nor, Tarim Basin.

2) only events after 04/01/76 are used.

Table 7. TG(ML8), $m_b(P_{max})$ and $m_b(P_b)$ vs. $m_b(P_a)$			
Site	$m_b(P_b)-m_b(P_a)$	$m_b(P_{max})-m_b(P_a)$	#[1]
BSW	0.290±0.012	0.524±0.013	14
BTZ	0.290±0.021	0.503±0.035	8
BNE	0.268±0.018	0.493±0.025	9
Deg	0.289±0.012	0.515±0.014	21
Mzk	0.300±0.017	0.531±0.020	13
KTS	0.289±0.006	0.516±0.008	65
NNZ	0.226±0.008	0.396±0.009	28
PRC	0.133±0.042	0.328±0.063	12

1) all events used.

Before Bocharov *et al.* (1989) published the yields and other source information of historical Soviet events, several attempts had been made to investigate the characteristics of cratering explosions in that region. For instance, McLaughlin *et al.* (1985) studied the ratio of the P_a phase and P_{max} phase of presumed Balapan contained and cratering explosions by comparing the WWSSN station m_b's. The motivation was that the logarithm of amplitude ratio of P_{max}/P_a of event 650115B was significantly smaller than other presumed contained explosions in the vicinity. Assuming the phase P_a is unaffected by the influence of the non-linear free-surface interference, then an adjustment to the $m_b(P_{max})$ should be able to convert that to a contained explosion of the same yield. McLaughlin *et al.* (1985) concluded that a correction between 0.17 and 0.27 is needed for this conversion, assuming a yield of 125KT.

Der *et al.* (1985) deconvolved four contained and the cratering Balapan events 650115B recorded at EKA, and then they convolved the Green's functions with an appropriate attenuation operator as well as the source-time function of various yields of interest. By comparing the phases P_a and P_{max} of the synthetics, they obtained a cratering-to-contained correction of 0.15, 0.15, and 0.18 at 60, 125, and 300KT, respectively.

Day *et al.* (1986) did a theoretical study with nonlinear source calculations to account for coupling variations with depth. Their results are summarized as follows:

$$m_b(\text{contained}) - m_b(\text{cratering}) \approx -(0.1 \text{ to } 0.15) \text{ direct coupling} + (0.1 \text{ to } 0.25) \text{ surface interaction effects} \approx (0 \text{ to } 0.15) \text{ total bias.}$$

Based on 46 Balapan explosions recorded at EKA, Ringdal and Marshall (1989) derived a value of 0.75 as their mean $\log(P_{max}/P_a)$ across the EKA array using the same techniques as used in McLaughlin *et al.* (1985). The cratering event 650115B had $m_b(P_{max}) - m_b(P_a) = 0.62$ at EKA, and hence they apply a correction of 5.87 + (0.75 - 0.62) = 6.00 for a hypothetical contained explosion with equivalent yield.

We utilize the statistics in Tables 6 through 9 to illustrate that the correction by Ringdal and Marshall (1989) might be slightly more accurate than that in the other studies cited above. For event 650115B, our $m_b(P_{max}) - m_b(P_a) = 0.392$ (Table 1), which is 0.123 m.u. lower than the average $m_b(P_{max}) - m_b(P_a) = 0.515$ (KTS) or 0.516 (BTZ, where this event is located) shown in Table 6. This implies a corrected $\overline{m}_{2.9}$ for contained 111 KT as 5.988±0.013. Alternatively, using Equations [6] and [8], we expect the $m_b(P_{max}) - m_b(P_a)$ to be 0.497 and 0.490 m.u. at 100 and 150 KT, respectively. This would imply a correction of about 0.1 m.u. associated with the range of 100-150 KT.

The cratering-to-contained conversions cited above typically require extra information about the general behavior of contained explosions in the same source region. For the purpose of estimating the yield of a cratering shot in an isolated region, using P_a could be a much easier approach.

Table 8 lists the expected m_b values for each of P_a, P_b, and P_{max} phases from NTS, NNZ, and KTS explosions based on Equations [6] and [8]. The estimated "mean" $\overline{m}_{2.9}$ bias can then be computed in a straightforward manner (Table 9). The bias estimates based on $\overline{m}_{2.2}$ are included for comparison.

Table 8. Expected m_b at Various Sites								
	$\overline{m}_{2.2}$				$\overline{m}_{2.9}$			
Phase/Site	1KT	10KT	50KT	100KT	1KT	10KT	50KT	100KT
$m_b(P_{max})$ (KTS)	4.270	5.080	5.646	5.890	4.399	5.167	5.704	5.935
$m_b(P_b)$ (KTS)	4.018	4.848	5.428	5.678	4.130	4.930	5.489	5.730
$m_b(P_a)$ (KTS)	3.735	4.560	5.137	5.385	3.834	4.636	5.197	5.438
$m_b(P_{max})$ (NNZ)[1]	4.254	5.019	5.554	5.784	4.245	5.040	5.596	5.835
$m_b(P_b)$ (NNZ)[1]	3.948	4.785	5.371	5.623	3.989	4.835	5.426	5.681
$m_b(P_a)$ (NNZ)[1]	3.735	4.560	5.137	5.385	3.834	4.636	5.197	5.438
$m_b(P_{max})$ (NTS)	3.749	4.608	5.208	5.467	3.954	4.771	5.342	5.588
$m_b(P_b)$ (NTS)	3.479	4.349	4.957	5.219	3.674	4.505	5.086	5.336
$m_b(P_a)$ (NTS)	3.368	4.186	4.758	5.004	3.607	4.372	4.907	5.137

1) from Jih and Wagner (1992).

Table 9. Expected m_b Bias Relative to NTS								
	$\overline{m}_{2.2}$				$\overline{m}_{2.9}$			
Phase/Site	10KT	50KT	100KT	150KT	1CKT	50KT	100KT	150KT
$m_b(P_{max})$ (KTS)	0.47	0.44	0.42	0.41	0.40	0.36	0.35	0.34
$m_b(P_b)$ (KTS)	0.50	0.47	0.46	0.45	0.42	0.40	0.39	0.39
$m_b(P_a)$ (KTS)	0.37	0.38	0.38	0.38	0.26	0.29	0.30	0.31
$m_b(P_{max})$ (NNZ)[1]	0.41	0.35	0.32	0.30	0.27	0.25	0.25	0.24
$m_b(P_b)$ (NNZ)[1]	0.44	0.41	0.40	0.40	0.33	0.34	0.35	0.35
$m_b(P_a)$ (NNZ)[1]	0.37	0.38	0.38	0.38	0.26	0.29	0.30	0.31

1) from Jih and Wagner (1992).

Marshall *et al.* (1984) found that explosions in the northeast and southwest portions of Balapan test site produce distinctly different waveforms when recorded at the UK seismological array stations, suggesting that Balapan test site can be subdivided into two areas

characterized by different geophysical properties. Ringdal and Hokland (1987) find that this pattern is persistently present whether m_b based on worldwide network or m_b(*P*coda) of NORSAR is used. They inferred the average m_b–L_g between SW and NE subregions as 0.17 m.u. In a follow-up study, Ringdal and Fyen (1988) suggest that there appear to be a transition zone between the NE and SW subregions. Ringdal and Marshall (1989) recomputed the SW-NE bias as 0.15 m.u. with 96 Balapan events recorded at ISC stations and NORSAR. Although Ringdal and Marshall (1989) agree that the possibility of a $m_b(L_g)$ bias contributing to this difference between SW and NE cannot be entirely ruled out, they tend to believe that this bias is due to a relative m_b bias between these two areas.

We followed the zoning in Ringdal and Marshall (1989) in partitioning Balapan test site into three regions: southwest (SW), transition zone (TZ), and northeast (NE). The m_b–L_g value of 0.11 m.u. shown in Table 10 is slightly smaller than that of previous studies, suggesting that our $\overline{m}_{2.9}(P_{max})$ may be somewhat better than other m_b. Regressions with yields published by Bocharov *et al.* (1989) show that NE explosions have positive L_g residuals and negative m_b residuals, whereas SW explosions show the opposite trend (Figure 19). Thus it would seem plausible that the apparent m_b–L_g bias could have been "enhanced" by the negative correlation between m_b and L_g residuals. It is interesting to note the much smaller m_b–L_g bias when P_a is used (Table 10). A three-dimensional geological model of the Balapan test site by Leith and Unger (1989) shows a distinct difference between the NE and SW portions of the test site, with the granites closer to the surface and the alluvium thinner in the southwest. The thicker alluvium layer in NE region could increase the waveform complexity and reduce the magnitudes measured with P_{max}. Nevertheless, the first motion (*i.e.*, P_a) should be least affected by this factor, and therefore a favorable source measure --- so long as it is not contaminated by the microseismic noise at the receiver site.

Nuttli (1987, 1988) suggests that there is a m_b bias of about 0.2 m.u. between Degelen and Balapan, with Degelen explosions having even larger m_b excitation (relative to L_g). We do not see such Degelen-Balapan bias with *RMS* L_g measured at NORSAR (Table 10). The Degelen data set alone is too small for decisive conclusion. However, if we treat Murzhik as part of Degelen, as did Nuttli (1987), the average $m_b(P_{max})$–*RMS* L_g(NORSAR) bias between Degelen and Balapan is only 0.02 m.u., which is insignificant.

Table 10. $\bar{m}_{2.9}$-*RMS* L_g(NORSAR) at Various Sites			
Site	$m_b(P_a)-m_b(L_g)$, #	$m_b(P_b)-m_b(L_g)$, #	$m_b(P_{max})-m_b(L_g)$, #
BSW	-0.504±0.011 11	-0.228±0.011 11	+0.023±0.015 20
BTZ	-0.523±0.045 6	-0.243±0.020 6	-0.041±0.015 14
BNE	-0.565±0.023 8	-0.304±0.014 9	-0.092±0.012 14
Deg	-0.484±0.046 5	-0.207±0.042 5	+0.012±0.034 5
Mzk	-0.562±0.073 3	-0.259±0.045 3	-0.046±0.032 3
KTS	-0.524±0.013 33	-0.250±0.010 34	-0.026±0.010 56
NNZ	-0.519±0.020 14	-0.296±0.023 14	-0.121±0.024 14

Table 11. $\bar{m}_{2.9}$-$m_b(L_g)$ (Nuttli) at Various Sites			
Site	$m_b(P_a)-m_b(L_g)$, #	$m_b(P_b)-m_b(L_g)$, #	$m_b(P_{max})-m_b(L_g)$, #
BSW	-0.544±0.050 8	-0.244±0.040 8	-0.034±0.028 16
BTZ	-0.444±0.078 5	-0.184±0.057 5	-0.033±0.024 13
BNE	-0.584±0.043 6	-0.303±0.039 7	-0.075±0.031 14
Deg	-0.524±0.124 5	-0.196±0.112 5	+0.050±0.100 5
KTS	-0.529±0.033 24	-0.239±0.028 25	-0.037±0.017 48
NNZ	-0.549±0.033 24	-0.324±0.035 24	-0.151±0.032 24

We suggest that the m_b–L_g bias between SW and NE Balapan can be tentatively decomposed into several parts:

[I] Difference in *pP* between SW and NE,

[II] Difference in m_b coupling, *i.e.*, m_b(SW) > m_b(NE),

[III] Difference in L_g coupling, *i.e.*, L_g(NE) > L_g(SW),

[IV] Effects due to the station-station correlation structure,

[V] Effects due to the uneven geographical clustering of stations, as well as any path effect which is not fully accounted for through the network averaging.

Based on our $\overline{m}_{2.9}$, [I] is about 0.05 m.u., whereas [II] and [III] are about 0.02-0.03 m.u. each. The bias of 0.11 m.u. in Table 10 using $m_b(P_{max})$ is the sum of [I] through [III]. It reduces to 0.06 if m_b based on the first motion is used, which reflects the sum of [II] and [III]. For ISC data, we estimate that [V] is about 0.02 m.u. if $\overline{m}_{2.2}$ derived by the conventional LSMF are used. When $\overline{m}_{2.9}$ is used, this term is eliminated, and hence a smaller m_b–L_g bias is obtained. [II] and [III] can be easily illustrated with regressions on Bocharov's published yields, as explained earlier (Figure 19). There are only a handful Balapan events with published yields in Bocharov *et al.* (1989). However, the 5 large historical events (for which the yields were exchanged during JVE) can also provide some further clue in support of our postulated hypotheses [I] through [III]. The yield estimate based on P_{max} for the three historical events in SW subregion (790804B, 791223B, and 811018B) is systematically larger than that based on P_a. On the other hand, the two events in NE subregion (791028B and 840526B) have smaller yield estimate based on P_{max} as compared to P_a. The larger bias of 0.15 m.u. that Ringdal *et al.* (1992) obtained with m_b(ISC) could have been "enhanced" by [IV] and [V]. The m_b determination procedure presented in this study does not correct for [IV] either. However, the contribution of inter-station correlation alone is believed to be insignificant if WWSSN is used.

In Figure 20 we show the difference of path effects between BSW and BNE at each WWSSN station, which is a measure of the relative bias between BSW and BNE along each path. Positive symbols represent the stations where BSW events are enhanced relative to BNE events. ISC network is dominated by western European stations and hence the effect due to [V] would be more severe than that on WWSSN. Figure 21 shows the spatial pattern of m_b-L_g residuals of Semipalatinsk explosions based on Geotech's m_b values and RMS L_g values reported at NORSAR. There is a significant difference in the source medium across the Chinrau fault separating the northeastern and southwestern portion of Balapan test site, as reported by Ringal and Marshall (1989) and Marshall *et al.* (1984) as noted in Table 10. The mean m_b-L_g bias between SW and NE Balapan is about 0.11 m.u. Figure 21 also indicates that SW events near the edge of the test site tend to have larger L_g excitation (and hence negative m_b–L_g residual). Although this seems to be reasonable, we must be cautious as this interpretation is highly dependent on the accuracy of the location as well as the geological information.

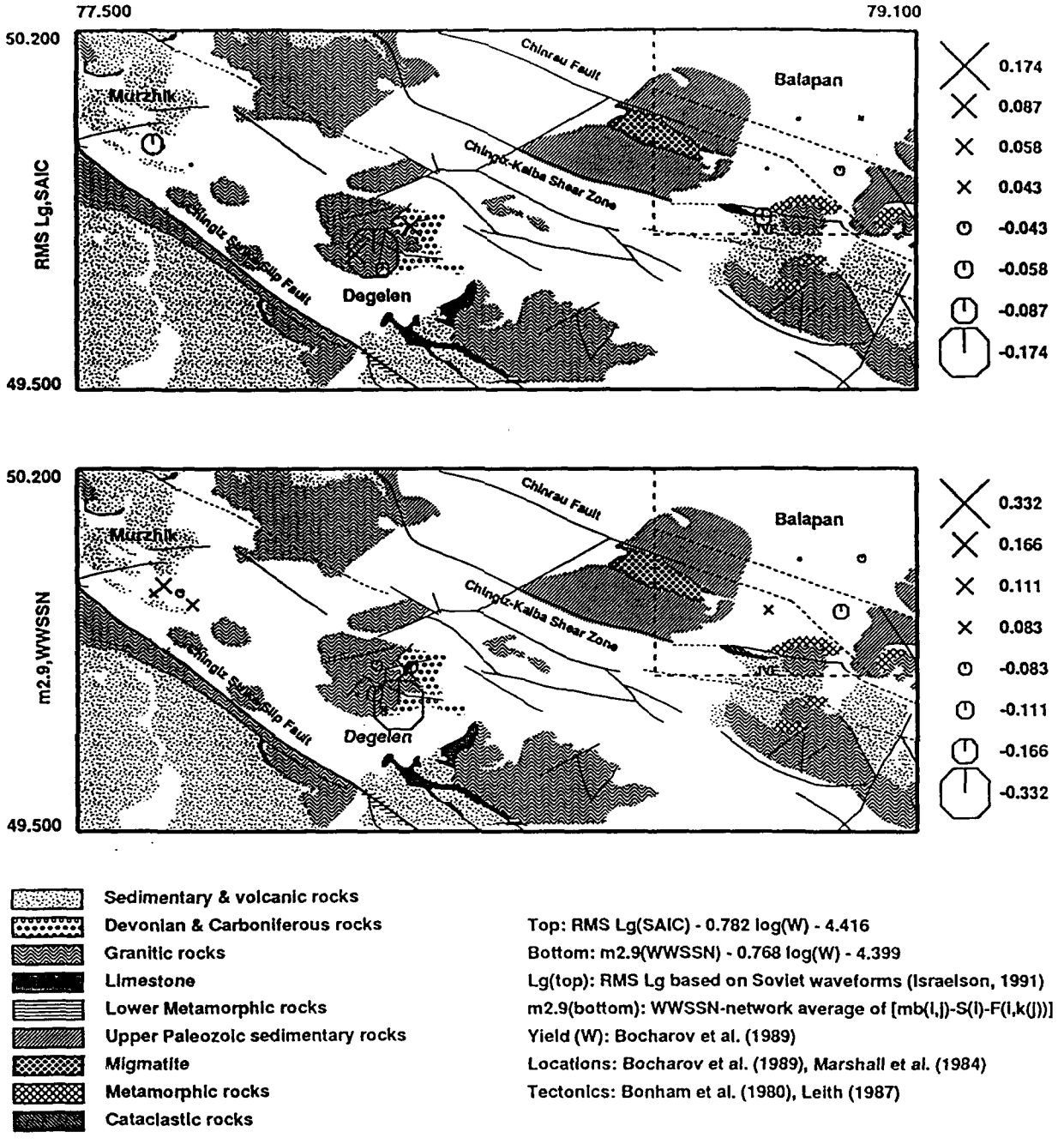

Figure 19. Regressions using yields published by Bocharov *et al.* (1989) indicate that BNE explosions have positive L_g residuals (top) and negative m_b residuals (bottom); whereas BSW explosions show the opposite trend. Thus it would seem plausible that the apparent m_b–L_g bias could have been "enhanced" by the negative correlation between m_b and L_g residuals. There is a distinct difference in the source media between the NE and SW portions of Balapan test site, with the granites closer to the surface and the alluvium thinner in the southwest. The thicker alluvium layer in NE region could increase the waveform complexity and reduce the magnitudes measured with P_{max}.

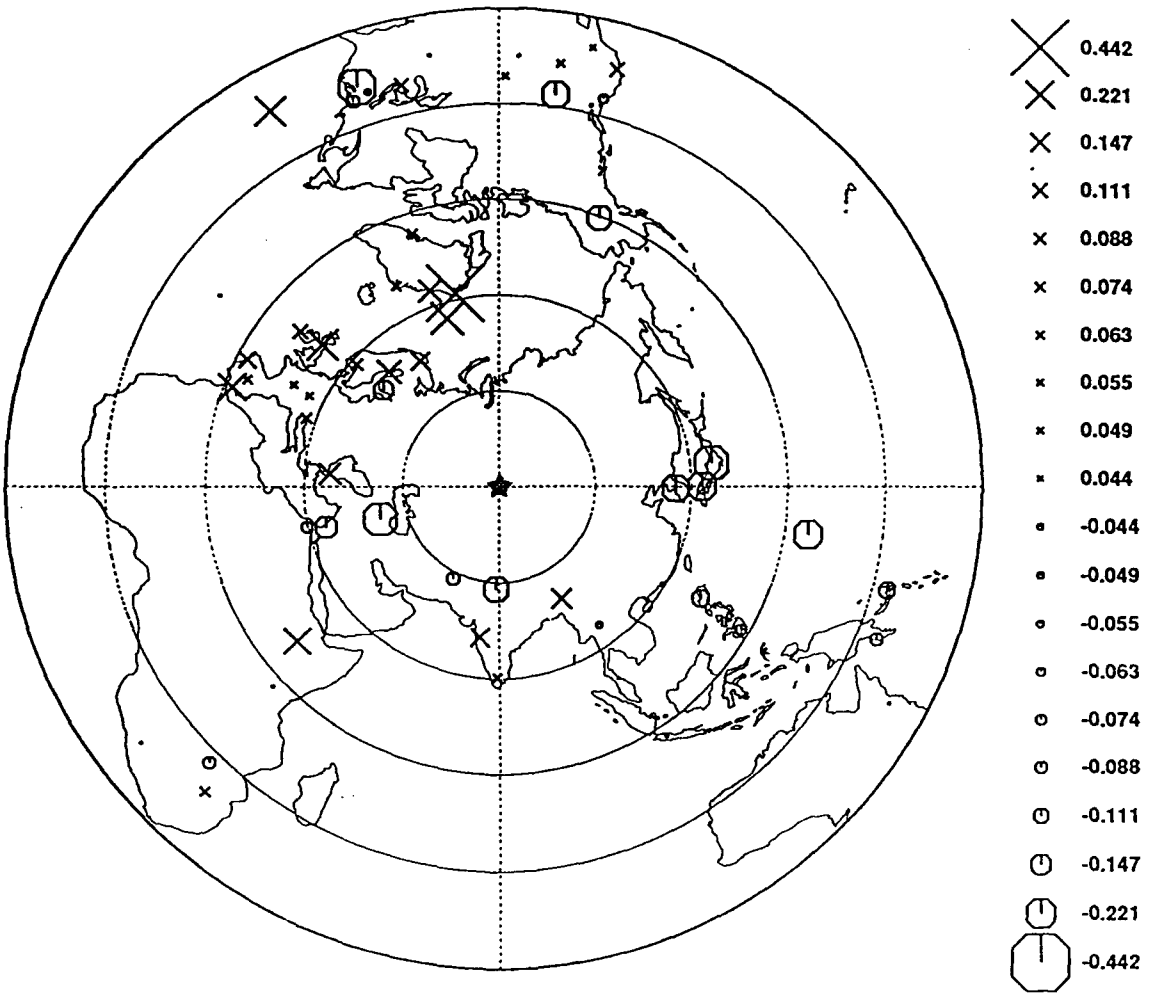

Figure 20. Averaged SW-NE bias at each WWSSN station. Positive symbols represent the stations where amplitude of BSW events is enhanced relative to that of BNE events of the same source strength. This pattern reflects the difference of path effects on these two adjacent test sites. For network with an uneven geographical distribution of stations (such as ISC), the simple network averaging of station magnitudes can only eliminate the path effect to certain extent.

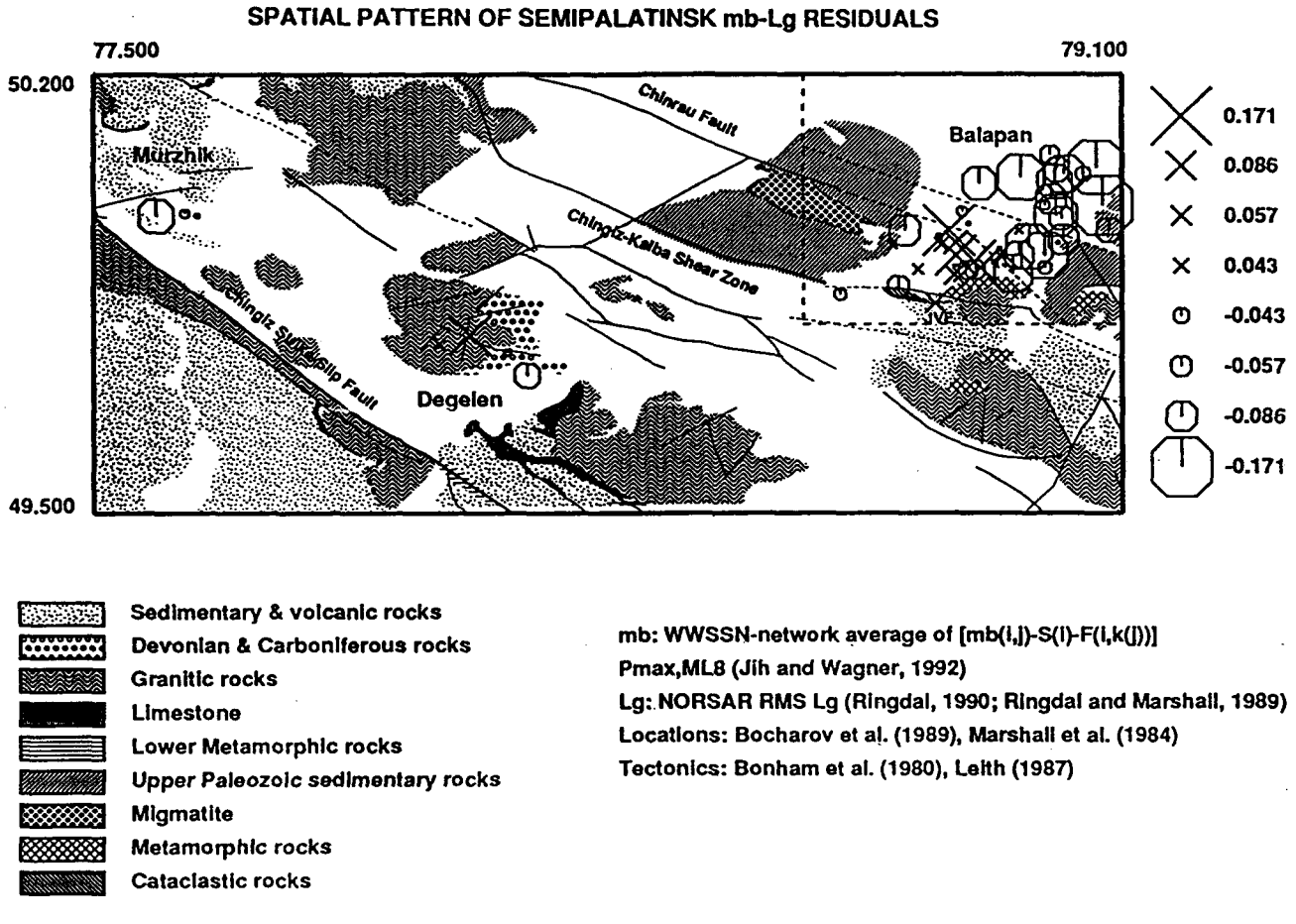

Figure 21. The spatial pattern of m_b-L_g residuals of Semipalatinsk explosions with TG's m_b(GLM) and RMS L_g values reported at NORSAR. The residual pattern of Balapan events strongly indicates significant difference in the source medium across the Chinrau fault separating the northeastern and southwestern portion of the test site, as reported by Ringal and Marshall (1989) and Marshall *et al.* (1984). The mean m_b-L_g bias between SW and NE Balapan is about 0.11 m.u.

6. PRELIMINARY ASSESSMENT OF WWSSN'S REMOTE MONITORING CAPABILITY

The potential capability of a seismic network for monitoring a low threshold test ban treaty is a complex function of the source and path characteristics, network geometry, and the signal-to-noise threshold of the network's stations (Bratt, 1991). Ringdal (1990b) conducted a study of the NORESS array detection capability for Semipalatinsk explosions. The 50% detection threshold at NORESS is estimated as m_b=3.7±0.1. Ringdal noted a large bias (of 0.6 m_b) between Balapan and Degelen/Murzhik subregions. Thus the actual NORESS detection threshold at 50% level is m_b=2.7 and 3.3 for Balapan and Degelen subregions. Ringdal (1990a) found subarrays of NORSAR have very different m_b residual patterns for Novaya Zemlya explosions, with m_b bias ranges from +0.9 (03C01) to -0.3 (01B05). For each WWSSN station, we computed the sum of its "averaged station effect" and the path term associated with each test site in Eurasian continent. A grading from A through E is then assigned to each station according to the magnitude of this combined "station amplification": A (excellent): 0.3 and larger; B (good): from 0.1 to 0.3; C (fair): from -0.1 to 0.1; D (acceptable): from -0.3 to -0.1; E (poor): -0.3 and smaller (Table 12).

Table 12. WWSSN's Capability in Monitoring Eurasian Explosions

Station	Lon	Lat	BSW	BNE	BTZ	DEG	MZK	AZG*	NNZ	PRC
AAE	38.766	9.029	E	E	E	E	E	D	C	---
AAM	-83.656	42.300	A	A	A	C	D	A	A	---
ADE	138.709	-34.967	---	---	---	-	---	---	-	B
AKU	-18.107	65.687	B	B	B	B	C	D	D	E
ALQ	-106.457	34.943	---	---	---	---	---	B	E	---
ANP	121.517	25.183	E	---	E	C	E	---	E	C
AQU	13.403	42.354	D	D	D	D	D	E	A	B
ATL	-84.338	33.433	---	---	---	---	---	C	C	---
ATU	23.717	37.972	B	B	B	D	C	E	B	A
BAG	120.580	16.411	D	C	D	D	D	B	B	E
BEC	-64.681	32.379	C	D	C	D	E	D	D	---

*) AZG: Azgir region, North Caspian.

Table 12. WWSSN's Capability in Monitoring Eurasian Explosions										
Station	Lon	Lat	BSW	BNE	BTZ	DEG	MZK	AZG	NNZ	PRC
BHP	-79.558	8.961	---	---	---	---	---	---	E	---
BKS	-122.235	37.877	C	C	C	C	B	B	C	---
BLA	-80.421	37.211	D	D	D	D	E	D	B	---
BOZ	-111.633	45.600	---	D	C	B	C	D	A	---
BUL	28.613	-20.143	D	C	C	E	C	C	A	D
CAR	-66.928	10.507	---	---	---	---	---	---	B	---
CHG	98.977	18.790	C	C	A	C	D	E	E	E
CMC	-115.083	67.833	---	---	D	B	B	---	D	---
COL	-147.793	64.900	C	B	B	C	C	B	C	B
COP	12.433	55.683	B	B	B	B	E	C	A	C
COR	-123.303	44.586	B	B	B	B	B	B	D	---
CTA	146.254	-20.088	C	C	B	C	C	---	---	D
DAG	-18.770	76.770	B	C	C	C	---	---	---	C
DAL	-96.784	32.846	---	---	---	---	---	A	B	---
DAV	125.575	7.088	E	E	E	E	---	---	D	E
DUG	-112.813	40.195	B	B	B	A	A	C	E	---
EIL	34.950	29.550	---	---	C	D	C	---	B	B
EPT	-106.506	31.772	---	---	---	---	---	---	D	---
ESK	-3.205	55.317	C	D	C	B	E	C	A	D
FLO	-90.370	38.802	---	---	D	D	E	C	C	---
FVM	-90.426	37.984	C	C	C	C	---	B	D	---
GDH	-53.533	69.250	C	C	C	D	C	D	E	B
GEO	-77.067	38.900	C	A	C	C	D	D	C	---
GOL	-105.371	39.700	C	C	C	C	D	C	E	---
GSC	-116.805	35.302	C	C	B	B	C	---	C	---
GUA	144.912	13.538	D	C	E	---	---	---	D	A
HKC	114.172	22.304	C	D	D	E	D	---	C	---
HLW	31.342	29.858	E	D	D	E	---	B	A	D
HNR	159.947	-9.432	C	---	---	---	---	---	---	---
IST	28.996	41.046	A	B	B	C	C	---	A	C

Table 12. WWSSN's Capability in Monitoring Eurasian Explosions										
Station	Lon	Lat	BSW	BNE	BTZ	DEG	MZK	AZG	NNZ	PRC
JCT	-99.802	30.479	---	---	---	---	---	---	C	---
JER	35.197	31.772	C	C	C	D	C	---	B	B
KBL	69.043	34.541	---	---	---	---	---	E	C	---
KBS	11.924	78.918	E	E	E	D	E	B	---	D
KEV	27.007	69.755	B	C	B	C	D	E	---	D
KIP	-158.015	21.423	---	---	---	---	---	---	B	---
KOD	77.467	10.233	A	A	B	B	A	C	C	E
KON	9.598	59.649	A	B	A	B	D	B	D	C
KRK	30.062	69.724	---	---	---	B	B	B	---	---
KTG	-21.983	70.417	D	D	C	D	D	E	E	---
LEM	107.617	-6.833	E	E	E	E	---	E	E	---
LON	-121.810	46.750	D	C	C	C	C	C	D	D
LOR	3.851	47.267	D	D	D	D	C	---	C	C
LPS	-89.162	14.292	---	---	---	---	---	---	C	---
LUB	-101.867	33.583	---	---	---	---	---	B	C	---
MAL	-4.411	36.728	B	C	C	C	D	E	B	---
MAN	121.077	14.662	---	A	A	B	---	---	B	---
MAT	138.207	36.542	E	E	E	E	E	E	E	E
MDS	-89.760	43.372	---	---	D	B	---	---	B	---
MSH	59.588	36.311	---	---	---	---	---	---	A	E
MSO	-113.941	46.829	D	C	C	D	---	C	D	C
MUN	116.208	-31.978	B	B	A	B	B	---	---	C
NAI	36.804	-1.274	D	D	D	D	D	D	C	C
NAT	-35.033	-5.117	---	---	---	---	---	---	D	---
NDI	77.217	28.683	C	B	C	B	B	B	B	---
NHA	109.212	12.210	---	---	---	D	E	---	---	---
NIL	73.252	33.650	---	---	---	---	---	---	C	---
NOR	-16.683	81.600	B	D	D	C	C	D	---	---
NUR	24.651	60.509	A	A	A	C	C	---	---	C
OGD	-74.596	41.088	D	D	D	E	E	C	D	---

Table 12. WWSSN's Capability in Monitoring Eurasian Explosions										
Station	Lon	Lat	BSW	BNE	BTZ	DEG	MZK	AZG	NNZ	PRC
OXF	-89.409	34.512	---	---	---	---	---	B	B	---
PDA	-25.663	37.747	C	C	C	D	---	C	B	---
PMG	147.154	-9.409	B	B	B	B	A	---	---	D
POO	73.850	18.533	B	C	C	B	B	E	D	D
PRE	28.190	-25.753	C	C	C	E	D	B	---	B
PTO	-8.602	41.139	D	E	D	E	D	C	C	D
QUE	66.950	30.188	E	D	E	E	E	E	E	E
RAB	152.170	-4.191	C	C	C	E	D	---	---	---
RCD	-103.208	44.075	A	B	C	B	---	---	A	---
SCP	-77.865	40.795	C	C	C	D	E	A	C	---
SDB	13.572	-14.926	---	C	B	C	B	---	C	E
SEO	126.967	37.567	E	C	D	E	E	E	C	D
SHA	-88.143	30.694	---	---	---	---	---	---	A	---
SHI	52.520	29.638	C	C	B	B	B	---	B	E
SHK	132.678	34.532	E	D	E	E	E	E	E	B
SHL	91.883	25.567	C	C	B	D	D	A	C	---
SJG	-66.150	18.112	---	---	---	---	---	---	E	---
SLR	28.282	-25.735	E	E	---	---	---	---	---	C
SNG	100.620	7.173	C	C	B	C	C	E	C	E
STU	9.195	48.772	C	C	C	B	B	C	C	D
TAB	46.327	38.068	B	A	A	B	A	---	B	A
TOL	-4.049	39.881	C	C	B	C	C	---	A	A
TRI	13.764	45.709	C	D	C	C	D	E	C	C
TRN	-61.403	10.649	---	---	---	---	---	B	B	---
TUC	-110.782	32.310	---	---	---	---	---	---	D	---
UME	20.237	63.815	A	A	A	C	C	C	---	D
UNM	-99.178	19.329	---	---	---	---	---	---	C	---
VAL	-10.244	51.939	C	C	C	C	D	D	B	C
WES	-71.322	42.385	D	E	D	E	E	E	D	B
WIN	17.100	-22.567	C	C	C	D	D	---	---	C

Nuttli (1986) used COP (Copenhagen, Denmark), KEV (Kevo, Finland), KON (Kongsberg, southern Norway), NUR (Nurmijarvi, Finland), and UME (Umea, Sweden) in measuring his $m_b(L_g)$ values for Balapan explosions. It is interesting to note that these five Scandinavian stations also give good or excellent *P*–wave recordings. Nuttli (1987) reported that none of COP, KEV, or KON have readable L_g amplitudes for the Degelen explosions he studied, although these stations do have readable L_g amplitudes for Balapan explosions of comparable worldwide network-averaged m_b. Our result also show that these three stations have larger amplification for *P* waves from Balapan explosions as compared to those from Degelen explosions.

Butler and Ruff (1980) examined SP *P*-wave amplitudes of Novaya Zemlya explosions recorded by WWSSN stations in U.S. The lowest amplitudes were found in GOL (Golden, Colorado) and ALQ (Albuquerque, New Mexico), with values a factor of 4 lower than the high amplitudes. Our study with an enlarged data set recorded at a global network shows a very consistent result. The stations showing the lowest amplitude are SHK (Shiraki, southern Honshu, Japan), KTG (Kap Tobin, eastern Greenland), GOL, SJG (San Juan, Puerto Rico region), LEM (Lembang, Java), and ALQ. On the other hand, COP (Copenhagen, Denmark), HLW (Helwan, United Arab Republic), MSH (Mashhad, Iran-Turkmenistan border), IST (Istanbul, Turkey), AQU (Aquila, central Italy), and ESK (Eskdalemuir, United Kingdom) report the highest amplitude for NNZ explosions. Note that the station COP, which has the largest combined station amplification, is also used in Nuttli's (1986, 1988) $m_b(L_g)$ study of Balapan and Novaya Zemlya events.

7. DISCUSSION AND CONCLUSIONS

Along with an extensive data set of worldwide explosions recorded at a global network, teleseismic body-wave amplitudes from 92 Semipalatinsk explosions are measured and analyzed to isolate the propagation characteristics and to derive a better measure of the source size. This new m_b factoring procedure reduces effectively the scatter in the station magnitudes across the network. For the extreme case, the variation reduction could reach a factor of about 3. In principle, it can be applied to other types of network-recorded magnitudes as well, such as $\hat{m_b}$ (the band-passed spectral amplitude, see Bache, 1982, and Murphy *et al.*, 1989), $m_b(L_g)$, M_o, and M_S.

We have recomputed the yield estimates of Semipalatinsk explosions based on the path-corrected m_b values derived in this study. Based on the first motion of the *P* wave alone, the (central-value) yield estimate of Soviet JVE (09/14/88) is 113 KT and that of the cratering event on 01/15/65 at Balapan test site is 111 KT, which are in excellent agreement with estimates derived by other means. Thus the first motion of the initial short-period *P* waves appears to be a very favorable source measure for explosions fired in hard rock sites underlain by the stable mantle (such as Semipalatinsk). The m_b bias relative to NTS at 50-KT level is inferred as 0.36 magnitude unit. Also included in this study are some preliminary assessment of WWSSN's capability in remotely monitoring Eurasian explosions. A strong correlation between the *P*–wave amplitude and L_g detection at teleseismic distance is observed.

Although our results can explain some of the propagation complexities in the initial *P*–wave arrivals, a follow-up study is needed to quantify further the contribution of near-source scattering to the waveform complexity in the *P* coda which is not covered in this study. Our previous modeling effort (McLaughlin and Jih, 1986, 1987, 1988; Jih and McLaughlin, 1988) of utilizing the linear finite-difference code (Jih *et al.*, 1988) focused on the effects of mountainous topography and hypothetical heterogeneity in the upper crust on teleseismic and regional phases with somewhat simplied structures of other test sites. We suggest that the follow-up research be accompanied with some well-constrained forward modeling study using more realistic structures of ex-Soviet test sites.

8. ACKNOWLEDGEMENTS

We thank Bob Blandford, Paul Richards, Peter Marshall, Bill Leith, and Alan Ryall for many helpful discussions. Wilmer Rivers reviewed and improved the manuscript. DARPA/CSS provided the WWSSN film chips used in this study. The PSLIB plotting library released by Paul Wessel (HIG) and Walter Smith (Scripps) has been used in preparing Figures 19 and 21. The geology shown in these two figures was re-digitized by Abdul Malik based on a map of Bonham *et al.* (1980). This research was supported under Phillips Laboratory contract F29601-91-C-DB23. The views and conclusions contained in this paper are those of the authors and should not be interpreted as representing the official policies, either expressed or implied, of the Defense Advanced Research Projects Agency or the U.S. Government.

9. REFERENCES

Bache, T. C. (1982). Estimating the yield of underground nuclear explosions, *Bull. Seism. Soc. Am.*, **72-6**, S131-168.

Bache, T. C., S. R. Bratt, and L. B. Bache (1986). *P*–wave attenuation, m_b bias, and the Threshold Test Ban Treaty, *Final Report SAIC-86/1647 for AFGL contract F19628-85-C-0021,* Science Applications International Corporation, San Diego, CA.

Barker, B. W. and J. R. Murphy (1988). Further studies of seismic variability at the Shagan River Test Site, *Report SSS-R-88-9213,* S-Cubed, Reston, VA.

Blandford, R. R. and R. H. Shumway (1982). Magnitude:yield for nuclear explosions in granite at the Nevada Test Site and Algeria: joint determination with station effects and with data containing clipped and low-amplitude signals, *Report VSC-TR-82-12,* Teledyne Geotech, Alexandria, Virginia.

Bocharov, V. S., S. A. Zelentsoz, and V. Mikhailov (1989). Characteristics of 96 underground nuclear explosions at the Semipalatinsk test site, *Atomic Energy,* **67**, 210-214

Bonham, S., W. J. Dempsey, J. Rachlin (1980). Geologic environment of the Semipalatinsk area, U.S.S.R. *(Preliminary Report),* U.S. Geological Survey, Reston, VA 22092.

Booth, D. C., P. D. Marshall, and J. B. Young (1974). Long and short period *P*–wave amplitudes from earthquakes in the range 0°-114°, *Geophys. J.*, **39**, 523-537.

Bratt, S. R. (1991). Global monitoring to low threshold: where we stand, *Proceedings of the*

13th DARPA/GL Seismic Research Symposium, 8-10 October 1991, Keystone, CO, (Eds J. Lewkowicz and J. McPhetres), *Report PL-TR-91-2208,* Phillips Laboratory, Hanscom Air Force Base, MA. **(ADA241325)**

Burdick, L. J. (1981). The changing results on attenuation of *P* waves, in *"A technical assessment of seismic yield estimation", Report DARPA-NMR-81-01, Appendix,* DARPA, Arlington, VA.

Butler, R. (1981). Estimation of body wave magnitudes and site specific propagation effects, in *"A technical assessment of seismic yield estimation", Report DARPA-NMR-81-01, Appendix,* DARPA, Arlington, VA.

Butler, R. and L. Ruff (1980). Teleseismic short-period amplitudes: source and receiver variations, *Bull. Seism. Soc. Am.*, **70-3**, 831-850.

Chang, A. C. and D. H. von Seggern (1980). A study of amplitude anomaly and m_b bias at LASA subarrays, *J. Geophys. Res.*, **85**, 4811-4828.

DARPA (1981). A technical assessment of seismic yield estimation, *Report DARPA-NMR-81-02,* DARPA/NMRO, Arlington, VA.

Dermengian, J. M., J. R. Murphy, and B. W. Barker (1986). A preliminary analysis of seismic variability at the Shagan River Test Site, *Report SSS-R-86-7580,* S-Cubed, Reston, VA.

Day, S. M., N. Rimer, T. G. Barker, E. J. Halda, and B. Shkoller (1986). Numerical study of depth of burial effects on the seismic signature of underground explosions, *Report DNA-TR-86-114 (=SSS-R-86-7398),* S-cubed, La Jolla, CA.

Der, Z. A., R. H. Shumway, A. C. Lees, and E. Smart (1985). Multichannel deconvolution of *P* waves at seismic arrays, *Report TGAL-85-04,* Teledyne Geotech, Alexandria, VA.

Douglas, A. (1966). A special purpose least squares programme, *AWRE Report No. O-54/66,* HMSO, London, UK.

Douglas, A., J. A. Hudson, and B. J. Barley (1981). Complexity of short-period *P* seismograms: what does scattering contribute? *AWRE Report No. O-3/81,* HMSO, London, UK.

Douglas, A., P. D. Marshall, P. G. Gibbs, J. B. Young, and C. Blamey (1973). *P* signal complexity re-examined, *Geophys. J. R. astr. Soc.*, **33,** 195-221.

Ericsson, U. (1971). A linear model for the yield dependent magnitudes measured by a seismograph network, *Report C4455-26,* Research Institute of National Defense, Stockholm, Sweden.

Evernden, J. F. and D. M. Clark (1970). Study of teleseismic *P*. II. Amplitude data, *Phys. Earth Planet. Interiors,* **4,** 24-31.

Evernden, J. F. and G. E. Marsh (1987). Yields of U.S. and Soviet nuclear tests, *Physics Today,* **8-1,** 37-44.

Gordan, M. R. (1988). *New York Times,* October 30, 137 P.A15.

Gutenberg, B. and C. F. Richter (1956). Magnitude and energy of earthquakes, *Annali Geofis,* **9,** 1-15.

Israelson, H. (1991). RMS magnitude and path corrections for USSR explosions *(abstract), EOS, Trans. A.G.U.*, **72-44**, 338.

Jih, R.-S. and K. L. McLaughlin (1988). Investigation of explosion generated SV L_g waves in 2-D heterogeneous crustal models by finite-difference method, *Report AFGL-TR-88-0025 (=TGAL-88-01),* Geophysics Laboratory, Hanscom Air Force Base, MA. **(ADA213586)**

Jih, R.-S., K. L. McLaughlin and Z. A. Der (1988). Free boundary conditions of arbitrary polygonal topography in a 2-D explicit elastic finite difference scheme, *Geophysics,* **53,** 1045-1055.

Jih, R.-S. and R. A. Wagner (1991a). Azimuthal variation of m_b residuals of E. Kazakh explosions and assessment of the path effects *(abstract), EOS, Trans. Am. Geophys. Union,* **72-17**, 193.

Jih, R.-S. and R. A. Wagner (1991b). Recent methodological developments in magnitude determination and yield estimation with applications to Semipalatinsk explosions, *Report PL-TR-91-2212(I) (=TGAL-91-05),* Phillips Laboratory, Hanscom Air Force Base, MA. **(ADA244503)**

Jih, R.-S. and R. A. Wagner (1992). Path-corrected body-wave magnitudes and yield estimates of Novaya Zemlya explosions, *Report PL-TR-92-2042 (=TGAL-91-09),* Phillips Laboratory, Hanscom Air Force Base, MA.

Jih, R.-S., R. A. Wagner, and R. H. Shumway (1991). Magnitude-yield regression with uncertain data: a Monte-Carlo approach with applications to Semipalatinsk explosions, *EOS, Trans. Am. Geophys. Union,* **72-44**, 338.

Jih, R.-S. and R. H. Shumway (1989). Iterative network magnitude estimation and uncertainty assessment with noisy and clipped data, *Bull. Seism. Soc. Am.*, **79,** 1122-1141.

Jih, R.-S., R. H. Shumway, D. W. Rivers, R. A. Wagner, and T. W. McElfresh (1990). Magnitude-yield relationship at various nuclear test sites: a maximum-likelihood approach using heavily censored yields, *Report GL-TR-90-0107 (=TGAL-90-03),* Geophysics Laboratory, Hanscom Air Force Base, MA. **(ADA223490)**

Johnson, L. R. (1981) Near-source effects on *P* waves, in *"A technical assessment of seismic yield estimation", Report DARPA-NMR-81-01, Appendix,* DARPA, Arlington, VA.

Leith, W. (1987a). Geology of NRDC seismic stations sites in Eastern Kazakhstan, USSR. *Open-File Report 87-597,* U.S. Geological Survey, Reston, VA 22092.

Leith, W. (1987b). Tectonics of Eastern Kazakhstan and implications for seismic source studies in the Shagan River area, *Proceedings of DARPA/FGL Annual Seismic Research*

Review, 34-37, 15-18 June, 1987, Nantucket, MA.

Leith, W. and J. Unger (1989). Three-dimensional geological modeling of the Shagan River nuclear test site, paper presented at *DARPA/AFTAC Annual Seismic Research Review,* Patrick AFB, FL.

Lilwall, R. C. and J. M. Neary (1985). Redetermination of earthquake body-wave magnitudes using ISC Bulletin data, *AWRE Report No. O-21/85,* HMSO, London, UK.

Lilwall, R. C., P. D. Marshall, and D. W. Rivers (1988). Body wave magnitudes of some underground nuclear explosions at the Nevada (USA) and Shagan River (USSR) Test Sites, *AWE Report O-15/88,* HMSO, London, UK.

Lynnes, C. S. and T. Lay (1990). Effects of lateral heterogeneity under the Nevada Test Site on short-period *P* wave amplitudes and travel times, *Pure and Applied Geophysics,* **132,** 245-267.

Marshall, P. D., D. Porter, and P. Peachell (1992). Analysis of seismograms from nuclear explosions of known yield at Degelen Mountain and Konystan in East Kazakhstan, USSR, *UK/AWE Report No. O-2/92,* HMSO, London, UK.

Marshall, P. D. and D. L. Springer (1976). Is the velocity of P_n an indicator of Q? *Nature,* **264,** 531-533.

Marshall, P. D., D. L. Springer, and H. C. Rodean (1979). Magnitude corrections for attenuation in the upper mantle, *Geophys. J. R. astr. Soc.*, **57,** 609-638.

Marshall, P. D., T. C. Bache, and R. C. Lilwall, R. C. (1984). Body wave magnitudes and locations of Soviet underground explosions at the Semipalatinsk Test Site, *AWE Report O-16/84,* HMSO, London, UK.

McLaughlin, K. L., and R.-S. Jih (1986). Finite-difference simulations of Rayleigh wave scattering by 2-D rough topography, *Report AFGL-TR-86-0269 (=TGAL-86-09),* Geophysics Laboratory, Hanscom Air Force Base, MA. **(ADA179190)**

McLaughlin, K. L., and R.-S. Jih (1987). Finite-difference simulations of Rayleigh wave scattering by 2-D shallow heterogeneity, *Report AFGL-TR-87-0322 (=TGAL-87-02),* Geophysics Laboratory, Hanscom Air Force Base, MA.

McLaughlin, K. L., and R.-S. Jih (1988). Scattering from near-source topography: teleseismic observations and numerical simulations, *Bull. Seism. Soc. Am.*, **78-4,** 1399-1414.

McLaughlin, K. L., I. N. Gupta, and R. A. Wagner (1985). Magnitude determination of cratering and non-cratering nuclear explosions, *Report TGAL-85-03,* Teledyne Geotech, Alexandria Laboratory, Alexandria, VA.

Minster, J. B., J. M. Savino, W. L. Rodi, T. H. Jordan, and J. F. Masso (1981). Three-dimensional velocity structure of the crust and upper mantle beneath the Nevada Test Site, *Report SSS-R-81-5138,* S-Cubed, La Jolla, California.

Murphy, J. R., B. W. Barker, and A. O'Donnell (1989). Network-averaged teleseismic *P*-wave spectra for underground explosions. Part I - Definitions and Examples, *Bull. Seism. Soc. Am.*, **79-1,** 141-155.

Murphy, J. R., J. L. Stevens, D. C. O'Neill, B. W. Barker, K. L. McLaughlin, and M. E. Marshall (1991). Development of comprehensive seismic yield estimation system for underground nuclear exploeions, *Report PL-TR-91-2161, Scientific Report #2,* Phillips Laboratory, Hanscom AFB, M.A.

Myasnikov, K. V., L. B. Prozorov, and I. E. Sitnikov (1970). Mechanical effects of single and multiple underground nuclear cratering explosions and the properties of the excavation dug by them, in *Nuclear Explosions for Peaceful Purposes* (I. D. Morokhov, Ed.), *Atomizdat, Moscow, LLL Report UCRL-Trans-10517,* 79-109.

North, R. G. (1977). Station magnitude bias --- its determination, causes, and effects, *Lincoln Laboratory, Technical Report 1977-24,* Massachusetts Institute of Technology, Lexington, MA.

Nuttli, O. W. (1986). L_g magnitudes of selected East Kazakhstan underground explosions, *Bull. Seism. Soc. Am.*, **76,** 1241-1251.

Nuttli, O. W. (1987). L_g magnitudes of Degelen, East Kazakhstan, underground explosions, *Bull. Seism. Soc. Am.*, **77,** 679-681.

Nuttli, O. W. (1988). Lg magnitudes and yield estimates for underground Novaya Zemlya nuclear explosions, *Bull. Seism. Soc. Am.*, **78,** 873-884.

Priestley, K. F., W. R. Walter, V. Martynov, and M. V. Rozhkov (1990). Regional seismic recordings of the Soviet nuclear explosion of the Joint Verification Experiment, *Geophys. Res. Lets.*, **17,** 179-182.

Richards, P. G. (1990). Progress in seismic verification of test ban treaties, *IEEE Technology and Society Magazine,* **9-4,** 40-52.

Richards, P. G., L. R. Sykes, and W. Tedards (1990). Evidence for reduced uncertainty in estimates of Soviet explosion yields, and for an increase in estimates of explosion detection capability (abstract), *EOS, Trans. A.G.U.*, **71-43**, 1477.

Ringdal, F. (1976). Maximum likelihood estimation of seismic magnitude, *Bull. Seism. Soc. Am.*, **66,** 789-802.

Ringdal, F. (1986). Study of magnitudes, seismicity, and earthquake detectability using a global network, *Bull. Seism. Soc. Am.*, **76,** 1641-1659.

Ringdal, F. (1990). NORSAR detection and yield estimation studies, in *Proceedings of the 12th DARPA/GL Seismic Research Symposium, 18-20 Sept 1990, Key West, FL,* (Eds J. Lewkowicz and J. McPhetres), *Report GL-TR-90-0212,* Geophysics Laboratory, Hanscom Air Force Base, MA. **(ADA226635)**

Ringdal, F. (1990). *P*–wave focusing effects at NORSAR for Novaya Zemlya explosions, in *NORSAR Basic Seismological Research, 1 Oct 1989 - 30 Sept 1990,* (S. Mykkeltveit, ed.), *Report GL-TR-90-0330,* Geophysics Laboratory, Hanscom AFB, MA.

Ringdal, F. and J. Fyen (1988). Comparative analysis of NORSAR and Grafenberg L_g magnitudes for Shagan River explosions, Semiannual Technical Summary, 1 Apr 1988 - 30 Sept 1988, *NORSAR Scientific Report No.1-88/89,* NTNF/NORSAR, Kjeller, Norway (Oct 1988).

Ringdal, F. and B. K. Hokland (1987). Magnitude of large Semipalatinsk explosions using *P* coda and L_g measurements at NORSAR, Semiannual Technical Summary, 1 April 1987 - 30 Sept 1987, *NORSAR Scientific Report No. 1-87/88,* NTNF/NORSAR, Kjeller, Norway.

Ringdal, F., P. D. Marshall, and R. Alewine (1992). Seismic yield determination of Soviet underground nuclear explosions at the Shagan River Test Site, *Geophys. J. Int.,* **109,** 65-77.

Rodean, H. C. (1979), ISC events from 1964 to 1976 at and near the nuclear testing ground in eastern Kazakhstan, *UCRL-52856,* Lawrence Livermore Laboratory, University of California, CA.

Solomon, S. and M. N. Toksoz (1970). Lateral variation of attenuation of *P* and *S* waves beneath the United States, *Bull. Seism. Soc. Am.*, **60,** 819-838.

Stump, B. W. (1991). Nuclear explosion seismology: verification, source theory, wave propagation and politics, *Review of Geophysics (Supplement), 734-741, April 1991, U.S. National Report to International Union of Geodesy and Geophysics 1987-1990,* American Geophysical Union, Washington D.C.

Sykes, L. R. and G. Ekstrom (1989). Comparison of seismic and hydrodynamic yield determinations for the Soviet joint verification experiment of 1988, *Proc. Natl. Acad. Sci. USA,* **86,** 3456-3460.

Sykes, L. R. and S. Ruggi (1989). Soviet nuclear testing, in *Nuclear Weapon Databook* (Volume IV, Chapter 10), Natural Resources Defense Concil, Washington D. C.

Veith, K. F. and G. E. Clawson (1972). Magnitude from short-period *P*–wave data, *Bull. Seism. Soc. Am.*, **62,** 435-452.

Vergino, E. S. (1989). Soviet test yields, *EOS, Trans. A.G.U.*, Nov 28, 1989.

von Seggern, D. H. (1973). Joint magnitude determination and analysis of variance for explosion magnitude estimates, *Bull. Seism. Soc. Am.*, **63,** 827-845.

von Seggern, D. and D. W. Rivers (1978). Comments on the use of truncated distribution theory for improved magnitude estimation, *Bull. Seism. Soc. Am.*, **68,** 1543-1546.

DISTRIBUTION LIST

NON-GOVERNMENT CONTRACTORS

Prof. Thomas Ahrens
Seismological Lab, 252-21
Div. of Geol. & Planetary Sciences
California Institute of Technology
Pasadena, CA 91125

Dr. Thomas C. Bache, Jr.
Dr. Thomas J. Sereno, Jr.
Science Applications Int'l Corp.
10260 Campus Point Drive
San Diego, CA 92121 (2)

Dr. Peter Basham
Dr. Robert North
Earth Physics Branch
Geological Survey of Canada
1 Observatory Crescent
Ottawa, Ontario,CANADA K1A OY3

Dr. Douglas R. Baumgardt
Dr. Zoltan A. Der
ENSCO, Inc.
5400 Port Royal Road
Springfield, VA 22151-2388

Prof. Jonathan Berger
IGPP, A-025
Scripps Institution of Oceanography
University of California, San Diego
La Jolla, CA 92093

Dr. G. A. Bollinger
Department of Geological Sciences
Virginia Polytechnic Institute
21044 Derring Hall
Blacksburg, VA 24061

The Librarian
Dr. Jerry Carter
Dr. Stephen Bratt
Center for Seismic Studies
1300 North 17th Street, Suite 1450
Arlington, VA 22209-2308 (3)

Michael Browne
Teledyne Geotech
3401 Shiloh Road
Garland, TX 75041

Dr. Lawrence J. Burdick
Woodward-Clyde Consultants
566 El Dorado Street
Pasadena, CA 91109-3245

Dr. Theodore Cherry
Science Horizons, Inc.
710 Encinitas Blvd, Suite 200
Encinitas, CA 92024 (2)

Dr. Kin-Yip Chun
Geophysics Division
Physics Department
University of Toronto
Ontario, CANADA M5S IA7

Dr. Paul M. Davis
Dept. Earth & Space Sciences
University of California (UCLA)
Los Angeles, CA 90024

Prof. Steven Day
Department of Geological Sciences
San Diego State University
San Diego, CA 92182

Ms. Eva Johannisson
Senior Research Officer
National Defense Research Institute
P.O. Box 27322
S-102 54 Stockholm, SWEDEN

Dr. Mark D. Fisk
Mission Research Corporation
735 State Street
P.O. Drawer 719
Santa Barbara, CA 93102

Prof. Stanley Flatte
Applied Sciences Building
University of California
Santa Cruz, CA 95064

Dr. Roger Fritzel
Pacific Sierra Research
1401 Wilson Blvd., Suite 1100
Arlington, VA 22209

Dr. Holly K. Given
Inst. Geophys. & Planet. Phys.
Scripps Inst. Oceanography (A-025)
University of California - San Diego
La Jolla, CA 92093

Prof. Hans-Peter Harjes
Institute for Geophysik
Ruhr University/Bochum
P.O. Box 102148
463 Bochum 1, FRG

Prof. Donald V. Helmberger
Seismological Laboratory
Div. of Geol. & Planetary Sciences
California Institute of Technology
Pasadena, CA 91125

Prof. Eugene Herrin
Prof. Brian Stump
Inst. for the Study of Earth and Man
Geophysical Laboratory
Southern Methodist University
Dallas, TX 75275

Prof. Bryan Isacks
Prof. Muawia Barazangi
Cornell University
Department of Geological Sciences
SNEE Hall
Ithaca, NY 14850

Prof. Lane R. Johnson
Prof. Thomas V. McEvilly
Seismographic Station
University of California
Berkeley, CA 94720

Robert C. Kemerait
ENSCO, Inc.
445 Pineda Court
Melbourne, FL 32940

Prof. Brian L.N. Kennett
Research School of Earth Sciences
Institute of Advanced Studies
G.P.O. Box 4
Canberra 2601, AUSTRALIA

Dr. Richard LaCoss
MIT-Lincoln Laboratory
M-200B
P.O. Box 73
Lexington, MA 02173-0073

Prof. Fred K. Lamb
Univ. of Illinois
Department of Physics
1110 West Green Street
Urbana, IL 61801

Prof. Charles A. Langston
Geosciences Department
403 Deike Building
The Pennsylvania State University
University Park, PA 16802

Prof. Thorne Lay
Dr. Susan Schwartz
Institute of Tectonics
Earth Science Board
University of California, Santa Cruz
Santa Cruz, CA 95064

Prof. Arthur Lerner-Lam
Prof. Paul Richards
Prof. C.H. Scholz
Lamont-Doherty Geol. Observatory
of Columbia University
Palisades, NY 10964

Dr. Manfred Henger
Fed. Inst. for Geosci. & Nat'l Res.
Postfach 510153
D-3000 Hanover 51, FRG

Dr. Peter Marshall
Dr. Alan Douglas
Procurement Executive
Ministry of Defense
Blacknest, Brimpton
Reading FG7-4RS, United Kingdom

Dr. Randolph Martin, III
New England Research , Inc.
76 Olcott Drive
White River Junction, VT 05001

Dr. Bernard Massinon
Societe Radiomana
27 rue Claude Bernard
75005 Paris, FRANCE (2)

Dr. Gary McCartor
Prof. Henry L. Gray
Department of Physics
Southern Methodist University
Dallas, TX 75275

Dr. Keith L. McLaughlin
S-Cubed
P.O. Box 1620
La Jolla, CA 92038-1620

Dr. Pierre Mecheler
Societe Radioman
27 rue Claude Bernard
75005 Paris, FRANCE

Prof. Bernard Minster
Prof. John Orcutt
IGPP, A-025
Scripps Institute of Oceanography
University of California, San Diego
La Jolla, CA 92093

Prof. Brian J. Mitchell
Dr. Robert Herrmann
Dept. of Earth & Atmospheric Sciences
St. Louis University
St. Louis, MO 63156

Mr. Jack Murphy
S-Cubed
11800 Sunrise Valley Drive
Suite 1212
Reston, VA 22091 (2)

Dr. Jay J. Pulli
Radix Systems, Inc.
2 Taft Court, Suite 203
Rockville, MD 20850

Dr. Frode Ringdal
Dr. Svein Mykkeltveit
NTNF/NORSAR
P.O. Box 51
N-2007 Kjeller, NORWAY (2)

Mr. Wilmer Rivers, Jr.
Teledyne Geotech Alexandria Laboratory
314 Montgomery Street
Alexandria, VA 22314-1581 (2)

Dr. Richard Sailor
TASC, Inc.
55 Walkers Brook Drive
Reading, MA 01867

Prof. Charles G. Sammis
Prof. Kei Aki
Center for Earth Sciences
University of Southern California
University Park
Los Angeles, CA 90089-0741

Prof. David G. Simpson
Lamont-Doherty Geological Observatory
of Columbia University
Palisades, NY 10964

Dr. Stewart W. Smith
Geophysics AK-50
University of Washington
Seattle, WA 98195

Prof. Clifford Thurber
Prof. Robert P. Meyer
University of Wisconsin-Madison
Department of Geology & Geophysics
1215 West Dayton Street
Madison, WS 53706

Prof. M. Nafi Toksoz
Prof. Anton Dainty
Earth Resources Lab
Mass. Institute of Technology
42 Carleton Street
Cambridge, MA 02142

Prof. Terry C. Wallace
Dept. of Geosciences
Building #77
University of Arizona
Tucson, AZ 85721

Dr. William Wortman
Mission Research Corporation
735 State Street
P.O. Drawer 719
Santa Barbara,CA 93102

U.S. GOVERNMENT AGENCIES

Mr. Alfred Lieberman
ACDA/VI-OA, Room 5726
320 21st Street, N.W.
Washington, D.C. 20451

Colonel Jerry J. Perizo
AFOSR/NP, Building 410
Bolling AFB
Washington, D.C. 20331-6448

Dr. Robert R. Blandford
AFTAC/CSS
1300 N. 17th Street, Suite 1450
Arlington, VA 22209

AFTAC/CA
(STINFO)
Patrick AFB, FL 32925-6001

Dr. Frank F. Pilotte
HQ AFTAC/TT
Patrick AFB, FL 32925-6001

Katie Poley
CIA-ACIS/TMC
Room 4X16NHB
Washington, D.C. 20505

Dr. Larry Turnbull
CIA-OSWR/NED
Washington, DC 20505

Dr. Ralph W. Alewine, III
Dr. Alan S. Ryall, Jr.
Ms. Ann U. Kerr
DARPA/NMRO
3701 N. Fairfax Drive
Arlington, VA 22303-1714 (7)

DARPA/OASB/Librarian
3701 N. Fairfax Drive
Arlington, VA 22303-1714

Dr. Dale Glover
DIA/DT-1B
Washington, D.C. 20301

Dr. Michael Shore
Defense Nuclear Agency/SPSS
6801 Telegraph Road
Alexandria, VA 22310

Dr. Max Koontz
U.S. Dept. of Energy/DP-5
Forrestal Building
1000 Independence Avenue
Washington, D.C. 20585

Defense Technical Information Center
Cameron Station
Alexandria, VA 22314 (2)

Dr. John J. Cipar, PL/GEPH
Phillips Lab/Geophysics Directorate
Hanscom AFB, MA 01731

James F. Lewkowicz, PL/GEPH
Phillips Lab/Geophysics Directorate
Hanscom AFB, MA 0l73l

Phillips Laboratory (PL/XO)
Hanscom AFB, MA 0l73l

Dr. James Hannon
Lawrence Livermore National Laboratory
P.O. Box 808
Livermore, Ca 94550 (2)

Office of the Secretary of Defense
DDR&E
Washington, D.C. 20330

Eric Chael
Division 924l
Sandia Laboratory
Albuquerque, NM 87l85

Dr. William Leith
U.S. Geological Survey
Mail Stop 928
Reston, VA 22092

Dr. Robert Masse
Box 25046, Mail Stop 967
Denver Federal Center
Denver, CO 80225

Dr. Robert Reinke
WL/NTESG
Kirtland, AFB, NM 87ll7-6008

(THIS PAGE INTENTIONALLY LEFT BLANK)